



Strain Potential of Liquefied Soil

Franklin R. Olaya, S.M.ASCE¹; and Jonathan D. Bray, F.ASCE²

Abstract: Several widely used field methods for estimating postliquefaction ground deformation are based on the laboratory data from one series of cyclic simple shear tests performed on one uniform clean sand reconstituted to three relative densities. It is not clear if the trends of this one data set are applicable to other clean sands, nonplastic silty sands, and nonplastic silts. A database of 579 test results on postliquefaction volumetric strain, including 299 test results that relate maximum shear strain to the factor of safety against liquefaction triggering, was compiled and used to examine trends for these soils. The database includes postcyclic test data on 10 clean sands, 2 gravels, 3 silty sands, 5 silts, and 3 clayey soils. The enlarged cyclic testing database was used to develop models that estimate postliquefaction volumetric strain and maximum shear strain as a function of soil type, state, and seismic demand. The models are applicable to uniform nonplastic soil. The state parameter was used in addition to relative density and void ratio to characterize the state of the soil. Correlations between these parameters enable the full data set to inform the models. **DOI: 10.1061/(ASCE)GT.1943-5606.0002896.** © 2022 American Society of Civil Engineers.

Author keywords: Cyclic tests; Liquefaction; Shear strain; State parameter; Volumetric strain.

Introduction

Saturated soil under cyclic loading accumulates shear strain that generates excess pore-water pressure that reduces effective stress. Depending on the intensity and duration of the cyclic loading, the generated excess pore-water pressure can trigger liquefaction. At a free-field level ground site, liquefaction triggering and the dissipation of the subsequent excess pore-water pressure in the soil produce volumetric strain resulting from sedimentation and reconsolidation processes. The accumulation of volumetric strain in the soil deposit leads to ground settlement that can damage structures, especially if differential. For sites with sloping ground or a freeface slope nearby, the accumulation of shear strain can produce lateral spreads. Lateral spreading of the ground is typically nonuniform, with great potential to damage infrastructure. The quantification of the likely amount of ground deformation resulting from these liquefaction effects is important. However, the processes involved in liquefaction-induced volumetric strain and shear strain accumulation in soil deposits are complex and often not captured by numerical simulations.

Empirical procedures are routinely used in engineering practice because they provide reliable estimates of the observed ground performance. Researchers have developed empirical procedures to estimate liquefaction-induced ground settlement and lateral movement using field case history data with models informed by the results of laboratory tests. To analyze trends in the data, the complex processes involved in liquefaction triggering and its consequences are captured using proxies that represent the state of the

Note. This manuscript was submitted on December 3, 2021; approved on June 1, 2022; published online on September 9, 2022. Discussion period open until February 9, 2023; separate discussions must be submitted for individual papers. This paper is part of the *Journal of Geotechnical and Geoenvironmental Engineering*, © ASCE, ISSN 1090-0241.

soil and the seismic demand. Widely used cone penetration test (CPT)-based empirical methods for estimating postliquefaction ground settlement and lateral spread displacement, such as those of Zhang et al. (2002) and Idriss and Boulanger (2008), are based on the set of liquefaction test data and family of curves developed by Ishihara and Yoshimine (1992). As shown in Fig. 1, the calculated factor of safety against liquefaction (FS_L) is used with an estimate of the initial relative density (D_r) of each layer of the liquefied soil to estimate the maximum shear strain (γ_{max}) potential, which is then used with D_r again to estimate the postliquefaction volumetric strain (ε_n) of each soil layer.

Lee and Albaisa (1974) and Nagase and Ishihara (1988) showed that ε_v increased systematically with increasing values of excess pore-water pressure ratio (r_u) up to a r_u of about 0.9. Once r_u reaches 1.0, volumetric strain is not correlated to r_u because ε_v continues to increase significantly once $r_u = 1.0$. Silver and Seed (1971), Youd (1972), and Tokimatsu and Seed (1987) satisfactorily used cyclic shear strain to estimate seismic-induced sand compression. Other researchers (e.g., Tatsuoka et al. 1984; Ishihara and Yoshimine 1992; Wu 2002) also found that γ_{max} correlates well with ε_v . Although other parameters have been proposed for estimating ε_n [e.g., the cumulative shear strain (Sento et al. 2004; Kazama 2011)], it is challenging to estimate reliably in a straightforward manner the shear strain-time history in forward analyses. Conversely, γ_{max} can be correlated to FS_L, which is routinely obtained in a liquefaction triggering assessment. Consequently, $\gamma_{\rm max}$ has been used widely in engineering practice to estimate ε_v . Therefore, test data are characterized in terms of ε_v and $\gamma_{\rm max}$ in this study.

The often-used Ishihara and Yoshimine (1992) data and relationships have provided key insights. They have formed a sound basis for the development of procedures to estimate liquefaction-induced shear strain and postliquefaction volumetric strain in clean sand deposits that respond like Fuji River sand. However, the Ishihara and Yoshimine (1992) data interpretation and family of curves were derived from one series of cyclic simple shear (CSS) tests performed on just one uniform clean sand reconstituted to three different relative densities (i.e., 47%, 73%, and 93%) and tested at one vertical effective confining stress (i.e., 196 kPa). It is not known if the relationships developed from test data on one uniform clean sand can be applied to other clean sands with other

¹Ph.D. Graduate Student Researcher, Dept. of Civil and Environmental Engineering, Univ. of California, Berkeley, CA 94720-1710 (corresponding author). ORCID: https://orcid.org/0000-0003-1896-912X. Email: folaya@berkeley.edu

²Professor, Dept. of Civil and Environmental Engineering, Univ. of California, Berkeley, CA 94720-1710. ORCID: https://orcid.org/0000-0001-9368-4365. Email: jonbray@berkeley.edu

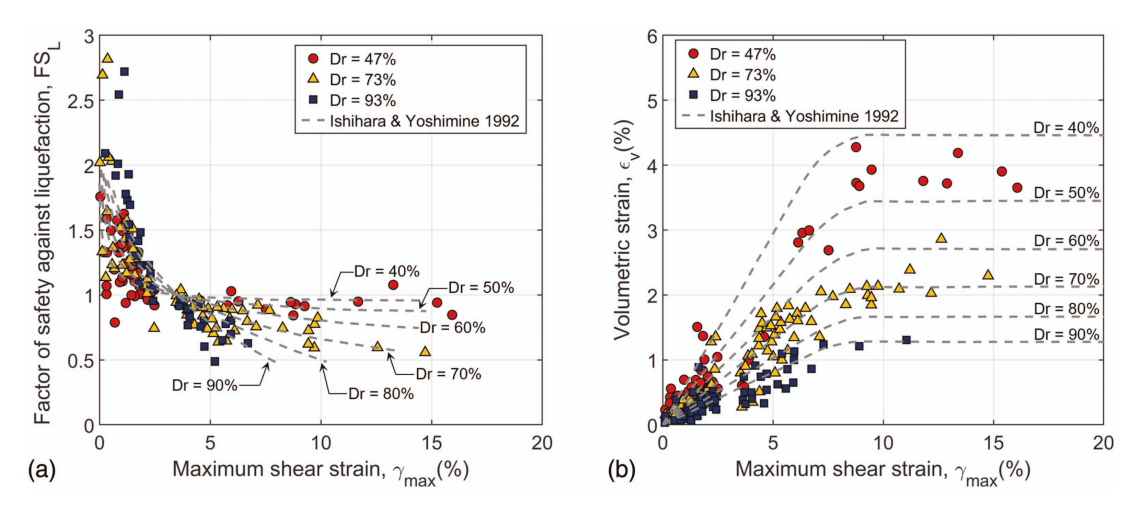


Fig. 1. (Color) Uniform clean sand. (Data from Ishihara and Yoshimine 1992.)

gradations, nonplastic silty sands, or nonplastic silts (e.g., Bray et al. 2017). Recognizing this issue, the examination of more experimental data is warranted. This is the primary motivation of this study.

A comprehensive laboratory database of maximum shear strain and postliquefaction volumetric strain from 10 clean sands, 2 gravels, 3 silty sands, 5 silts, and 3 clayey soils was compiled and interpreted. A subset of this enlarged database contained enough information to also interpret the relation of the factor of safety against liquefaction and maximum shear strain. The larger database enables the evaluation of trends of the variation of $\gamma_{\rm max}$, ε_v , and FS_L with other parameters, including three soil state indexes [the state parameter (ψ_o) , relative density, and void ratio (e_o)] for a wider range of soils than examined previously. The findings from this examination supports the development of new models relating γ_{max} , ε_v , and FS_L as a function of ψ_o , D_r , and e_o . A relationship to estimate ψ_o based on D_r is developed when it is not available. The models of cyclic-induced maximum shear strain and postliquefaction volumetric strain can be used to develop new liquefaction ground deformation procedures.

Strain Potential Laboratory Database

The laboratory data included in the expanded strain potential database contain information of grain-size distribution, initial void ratio or relative density, test type and conditions, and shear strain and volumetric strain measurements. Studies including cyclic resistance ratio (CRR) versus number of load cycles (N_c) for different shear strain levels were used to generate additional information on $\gamma_{\rm max}$ versus FS_L. The test results compiled for this study involve postliquefaction reconsolidation under either K_o or isotropic conditions. Once the cyclic shear stage was completed, the specimens were brought to a zero-lateral-strain equilibrium position to minimize residual strains within the specimen to capture free-field conditions and then drainage valves were opened to allow reconsolidation. Table 1 summarizes relevant index properties, such as particle gradation, fines content (FC), and plasticity index (PI), and test conditions such as test type, D_r , and vertical effective confinement pressure σ'_{vc} .

Specimen preparation and the applied cyclic stress ratio (CSR) were also recorded in the database, in addition to the measured $\gamma_{\rm max}$ and ε_v for each series of tests. Additional details of the compiled

database are provided in Table S1. Fig. 2 displays the range of grain-size distributions of the soils in the database.

The laboratory cyclic test database contains 579 $\gamma_{\rm max}$ - ε_v data points and 299 $\gamma_{\rm max}$ -FS $_L$ data points. Initially, the data sets on $\gamma_{\rm max}$ - ε_v for clean sand and gravel materials were examined. Then, nonplastic silty sand test data were evaluated, followed by nonplastic silt and low-plasticity silt. Lastly, the volumetric strain response of some clayey soils in cyclic testing was examined because laboratory tests on these materials indicated it is not zero. Like Ishihara and Yoshimine (1992) and several other researchers examining uniform sand data, D_r was employed to bin the data. Bolton (1986) showed that the shear response of different clean sands can be grouped and characterized using D_r provided these sands are of similar uniform gradations. Duncan et al. (2014) also showed D_r is an efficient parameter for characterizing the strength of granular materials of similar gradations represented by their coefficient of uniformity C_u .

Likewise, Whang (2001) analyzed seismically induced compression of different sands using D_r . Later, Duku et al. (2008) combined 16 different sands using D_r to develop a seismic recompression model of a broad range of uniform sands. Engineers often use D_r to characterize the state of a sand, and it is a primary parameter for several constitutive models for sand (e.g., Boulanger and Ziotopoulou 2015). Most of the test data in this study are of uniform clean sands ($C_u < 4.5$), with only some data on well-graded materials, which were used only to examine the effects of well-graded sands compared with uniform sands. Model development was restricted to uniform soils. In addition to D_r , e_o was employed, which is necessary for plastic soils. Lastly, there is merit to moving from using D_r to using ψ_o because it captures the interacting effects of soil density and confining stress. Thus, the data in which ψ_o could be estimated were interpreted in terms of the state parameter.

Volumetric Strain Potential in Terms of Relative Density

Volumetric Strain Response of Clean Sand

To evaluate whether all clean uniform sands should necessarily exhibit the same volumetric response to cyclic loading as Fuji River sand, D_r was used initially to characterize the state of the sand. As mentioned previously, D_r has often been used to characterize the state of uniform sand (e.g., Bolton 1986; Whang 2001;

Table 1. Liquefied soil strain potential laboratory test data

			Index properties				Test conditions		Number of tests		
ID	References	Test type	PI	C_u	FC (%)	USCS	Initial, D_r (%)	Confinement (kPa)	ε_v - γ_{\max}	$\gamma_{\max} - \mathrm{FS}_L$	Data class
1	Tatsuoka et al. (1984)	CTS	NP	2.4	~1	SP	55–86	196	12	_	A
2	Chin (1987)	CTX	NP	2.65	0	SP	60	74	16	_	В
3	Ishihara and Yoshimine (1992) ^a	CSS	NP	3.2	0	SP	47, 73, 93	196	200	164	A
4	Shamoto et al. (1996)	CTX	NP	1.55	0.1	SP	50	100	12	_	A
5	Wu (2002)	CSS	NP	1.3	0	SP	38-87	34-182	35	12	В
6	Sancio (2003)	CTX	2-25	2.3 - 3.6	68-100	CL, ML, MH	N/A	25-300	32	14	A
7	Tsukamoto et al. (2004)	Large CTX	NP	1.55	0	SP	60-80	98	43	38	A
8	Porcino and Caridi (2007)	CSS	NP	1.5	0	SP	40-75	100	2	_	В
9	Cetin et al. (2009)	CTX	NP	2.4	0	SP	35-85	100	35	_	В
10	Thevanayagam and Shenthan (2010)	CTX	NP	1.7	0	SP	32–81	100	6	_	A
11	Markham (2015)	CTX	2-5	1.9-8.3	3-93	SP-SM/ML	58-86	37-210	21	4	A
12	Parra (2016)	CSS	NP	1.6	<1	SP	24-85	50-404	14	_	В
13	Beyzaei (2017)	CTX	0–15	1.3-4.0	1–100	ML, CL, SP-SM	47–90	35–113	38	32	A
14	Hubler (2017)	Large CSS	NP	1.6	0	SP	50, 90	100	2	_	В
15	Toriihara et al. (2000)	CTX	NP	18	20	SM	72-112	N/A	25	11	D
16	Donahue (2007)	CTX	10	>30	77	CL	N/A	50	2	_	A
17	Wang and Luna (2014)	CTX	6	30	80	ML	N/A	90	12	_	C
18	Bilge (2010)	CTX	5-59	~60	39-97	ML-CH	N/A	N/A	41	_	В
19	Tsukamoto et al. (2004)	Large CTX	NP	35	8	GW-GM	65-90	98	29	24	A
20	Hubler (2017)	Large CSS	NP	1.6	0	GP	44, 81	100	2		В

Note: CTS = cyclic torsional shear; CSS = cyclic simple shear test; CTX = cyclic triaxial test; NP = nonplastic; and N/A = not available. alshihara and Yoshimine (1992) reinterpreted the test results first published by Nagase and Ishihara (1988).

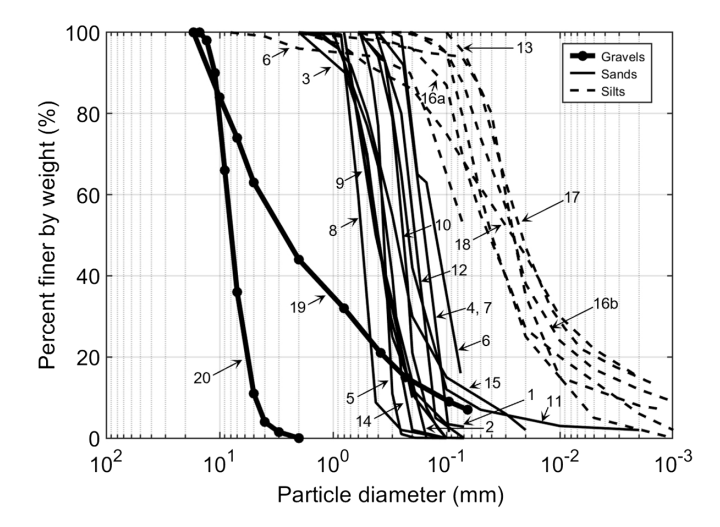


Fig. 2. Available grain-size distribution of soils in the database. Numbers indicate soil's ID in Table 1.

Duncan et al. 2014). Data from an additional nine clean uniform sands from different origins, formation processes, and gradations were collected and processed to produce 177 additional data points. The new data cover a wider range of D_r values ranging from 24% to 92%. The enlarged database provides a more robust basis for developing a generalized $\gamma_{\rm max}$ - ε_v model for clean uniform sand.

The data were subdivided into 10% bins of D_r to explore the influence of the sand's initial state on its postliquefaction response and to estimate mean (μ) values of ε_v and the uncertainty of this estimate for each bin. Hence, D_r was treated as an independent

variable in this part of the assessment. Eight D_r bins were generated, i.e., from 20%–30% to 90%–100%, with representative results shown in Fig. 3 where uniform sand γ_{max} - ε_v data are shown along with the Ishihara and Yoshimine (1992) data points in a lighter color for comparison.

Examination of the test data provides useful insights (Fig. S1 shows for more data than those in Fig. 3): (1) ε_v measurements have significant scatter for each bin of D_r ; (2) σ'_{vc} does not have a significant effect on ε_v over the range of $\sigma'_{vc} = 40$ –400 kPa; (3) isotropic reconsolidation (triaxial conditions) and K_o reconsolidation (one-dimensional conditions) produce similar amounts of ε_v (4) ε_v depends primarily on the induced $\gamma_{\rm max}$ and not the type of loading; (5) a direct relationship between ε_v and $\gamma_{\rm max}$ exists; (6) an inverse relationship between ε_v and $\gamma_{\rm max}$ exists; (6) an inverse relationship between ε_v and $\gamma_{\rm max}$ exists; (7) ε_v increases linearly with increasing $\gamma_{\rm max}$ up to a limiting shear stain of about $\gamma_{\rm max} = 7\%$ to 9%, after which ε_v remains relatively constant (within the limits of its inherent variability) at larger shear strain.

The dispersion of the ε_v measurements can be initially characterized by means of a simple linear regression performed over each D_r bin with the standard error of the estimate (standard error) used as the metric for comparison. If an individual uniform clean sand data set is analyzed (e.g., Ishihara and Yoshimine 1992), the standard error of the ε_v data with respect to the linear fit is usually less than 0.4%. When the results from tests on several uniform clean sands are combined, the standard error for each D_r bin of test data generally increases (e.g., 0.7% to 0.8%) showing that the variability in ε_v for a general clean uniform sand could easily be larger than implied in the original Ishihara and Yoshimine (1992) data set. Hence, the inclusion of several clean sand data sets enables more robust estimates of the general response of a generic uniform clean sand over a wider range of conditions (e.g., larger range

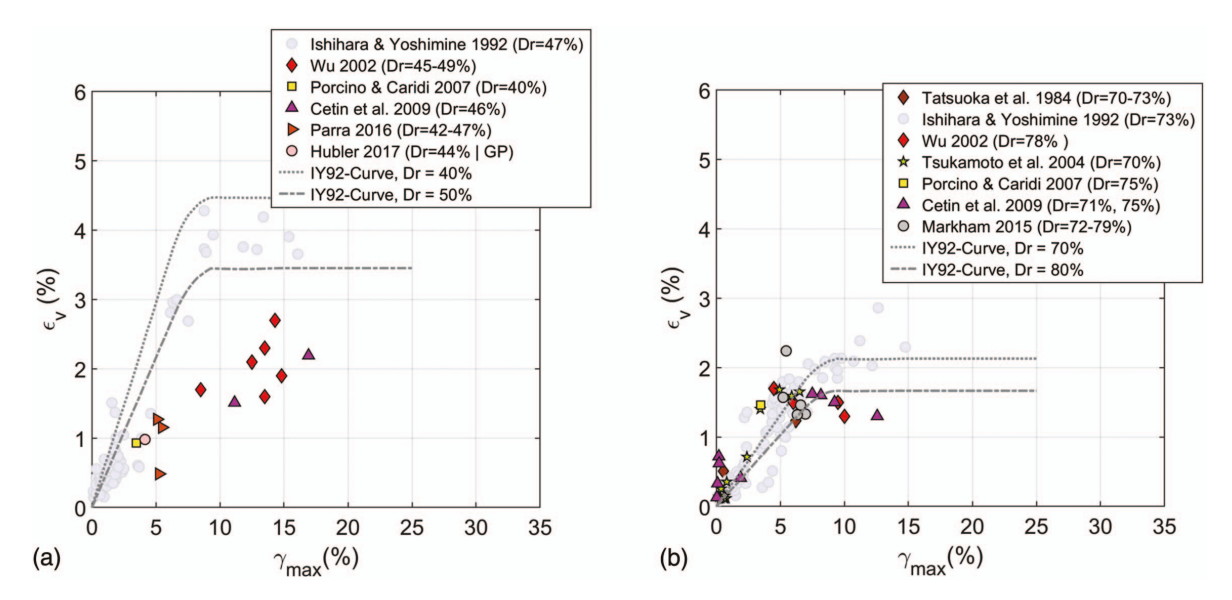


Fig. 3. (Color) Clean uniform sand ε_v - $\gamma_{\rm max}$ data for (a) $D_r = 40\% - 50\%$; and (b) $D_r = 70\% - 80$. Ishihara and Yoshimine (1992) data are shown in light blue for reference.

of D_r values) with a comprehensive characterization of the overall variability.

Importantly, the additional sand data also enable the identification of trends that emerge through combining the individual data sets. Despite the increased variability, the data of several uniform clean sands across the different D_r bins support a linear relationship between $\gamma_{\rm max}$ and ε_v up to $\gamma_{\rm max}\approx 7\%$ to 9%, and beyond $\gamma_{\rm max}\approx 9\%$, a ε_v plateau is observed. In addition, the larger data set indicates that the Ishihara and Yoshimine (1992) relationship slightly underestimates ε_v for high D_r ($\geq 70\%$) values [e.g., Fig. 3(b)]. Conversely, the Ishihara and Yoshimine (1992) relationship tends to overestimate ε_v for low D_r values ($\leq 50\%$). Hence, the development of an updated relationship that accounts for the observed variability is warranted.

Volumetric Strain Response of Nonplastic Silty Sand

Cubrinovski and Ishihara (2000) and Jefferies and Been (2016) showed, with all other conditions maintained, nonplastic fines increase the sand's compressibility, which reduces its penetration and cyclic resistance. Empirical liquefaction triggering methods deal with this difference in penetration resistance in more compressible nonplastic silty sand through an equivalent-clean-sand penetration resistance with the use of a fines content correction (e.g., Idriss and Boulanger 2008). This correction maps the penetration resistance of a silty sand to that of an equivalent-clean-sand so that the liquefaction evaluation can be performed in the clean sand domain where most of the adjustment factors to the cyclic resistance (e.g., magnitude scaling factor) have been developed. However, researchers have questioned whether this corrected equivalentclean-sand penetration resistance should be used directly with empirically based clean sand γ_{max} - ε_v models (e.g., Zhang et al. 2002; Bray et al. 2017). This issue warrants an examination of silty soil test data to better understand the postliquefaction response of silty soil.

Cubrinovski (2019) used D_r to examine field-based methods of liquefaction triggering of sands with different amounts of nonplastic fines. He found D_r of a high-FC soil can be used to assess the liquefaction potential of sand with fines, and it can be linked

directly to that of clean sand to aid in the interpretation of laboratory studies. Use of D_r enables one to explore if clean sands and nonplastic silty sands prepared at the same D_r under the same effective confining stress and sheared to the same $\gamma_{\rm max}$ develop similar ε_v . The maximum and minimum void ratio tests required to define D_r are typically reserved for soil with less than 5%–15% fines. However, Cubrinovski and Ishihara (2002) found that the Japanese Standard method yielded consistent e_{\min} and e_{\max} values for sands with nonplastic fines contents of up to 35%. Recently, Mijic et al. (2021a) obtained reasonable e_{\min} and e_{\max} values for nonplastic silty sand and nonplastic sandy silt with FC up to 70%. Moreover, their e_{\min} and e_{\max} values were not unreasonable for nonplastic silt up to 100% fines. Based on the findings of these studies, D_r is used to enable sand, nonplastic silty sand, and nonplastic silt data of uniform gradations to be compared and interpreted.

As noted in previous studies (e.g., Cubrinovski and Ishihara 2002; Thevanayagam et al. 2002), the maximum void ratio decreases with increasing FC from 0% to about 30%, and then increases at a higher rate with increasing FC beyond about 30%. A FC of about 30% marks the transition from a sand-dominated particle structure to a fines-dominated particle structure for nonplastic soil. If composed of similarly shaped particles of the same mineralogy with similar C_u values (i.e., similar compressibility), one might assume for practical purposes a uniform, fine clean sand (SP) responds similarly to a uniform nonplastic silty sand (SM) and to a uniform, coarse nonplastic silt (ML) if at the same D_r and confining stress. Significant changes in soil response are not expected for soils composed of uniform distributions of similarly shaped quartz particles that cross the No. 200 sieve at different points (Mijic et al. 2021b). Although the state parameter would be a better unifying index of the state of these soils, most data sets do not provide the steady state line (SSL). Hence, D_r is also used until more ψ_o data are available.

Fig. 4 shows data from Markham (2015) (FC = 6% to 12%) and Beyzaei (2017) (FC = 9% to 10%) corresponding to $D_r = 70\%$ –80%. The uniform silty sand ($C_u < 4.2$) test results are plotted in solid whereas uniform clean sand ($C_u = 1.5$ –3.2) data are plotted in lighter colors for comparison. These test results show

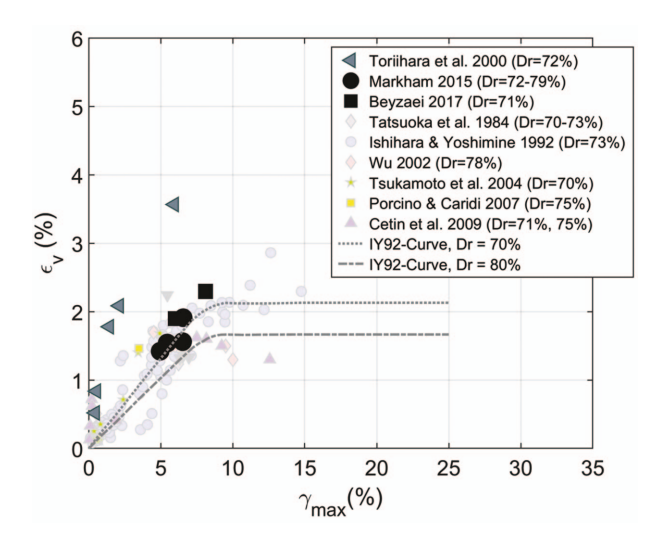


Fig. 4. (Color) Nonplastic to low-plasticity silty sand ε_v - $\gamma_{\rm max}$ data for $D_r=70\%$ -80%. Clean uniform sand data shown in light colors.

that uniform nonplastic silty sand and clean sand produced similar values of $\varepsilon_v=1.4\%$ to 2.3% at $\gamma_{\rm max}=5\%$ to 9%. Conversely, the Toriihara et al. (2000) well-graded silty sand data ($C_u=18$) differed significantly. The ε_v values in this test series were systematically higher than the other silty sand data and clean sand data. This is consistent with the extreme void ratios of this silty sand of $e_{\rm min}=0.94$ and $e_{\rm max}=1.53$, which are typical of compressible fine-grained soil.

Additionally, Tsukamoto et al. (2004) reported this sand could achieve D_r as high as 112%, which suggests grain crushing. Hence, it is likely that the unusually high ε_v values of the Toriihara et al. (2000) data set are due to the high compressibility of the fine matrix and some particle breakage upon shearing. The results of the Markham (2015) and Beyzaei (2017) uniform SM test data were consistent with the SP results discussed previously. The dispersion of the SM test data in each D_r bin is illustrated with the standard error of the linear model estimate, which varies from 0.35% to 0.75%. Data also show that the standard error increases significantly when the data are combined because there is little overlap in the smaller SM data set. Additional test results on silty sands are provided in the Fig. S2.

Volumetric Strain Response of Silt

Cubrinovski and Ishihara (2002) and Thevanayagam et al. (2002) found that the finer fraction controls particle fabric and response of soils with FC greater than about 30%, indicating that sands with FC greater than about 30% respond more like a silt than a clean sand. Herein, nonplastic silty sand with FC greater than about 30% are combined with the data on nonplastic silts classified using the Unified Soil Classification System (USCS) to examine the volumetric response of nonplastic silt. Bray and Sancio (2006), Beyzaei et al. (2018), Markham et al. (2018), and other researchers have shown that nonplastic silts liquefy in a manner similar to mediumdense angular clean sands in what is termed cyclic mobility. As discussed previously, D_r can be used to characterize the state of nonplastic silt data of uniform gradations (e.g., Mijic et al. 2021a, b).

Beyzaei (2017) reported a series of cyclic triaxial tests with postliquefaction reconsolidation measurements on Christchurch nonplastic silts with D_r ranging from 47% to 90%. A total of

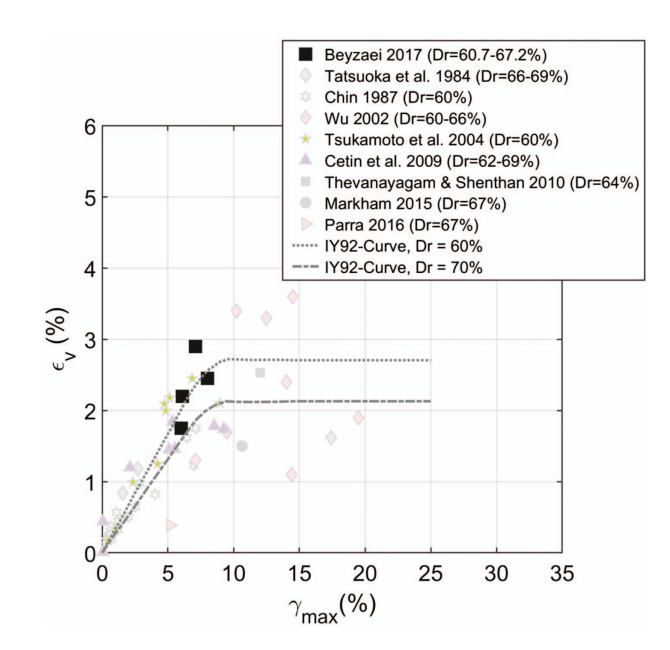


Fig. 5. (Color) Nonplastic uniform silt ε_v - $\gamma_{\rm max}$ data for $D_r = 60\%$ -70%. Clean uniform sand data shown in light colors.

11 $\gamma_{\rm max}$ - ε_v data points were collected from her study and plotted to compare with the larger clean sand data (Fig. S3). The standard error of the linear model estimate of the limited Beyzaei (2017) ML test data is 0.20% to 0.60%. A subset of Beyzaei (2017) data is presented in Fig. 5 with the clean sand data discussed previously shown in lighter colors for $D_r = 60\%$ -70%.

The results indicate the uniform nonplastic silt reconsolidated similar amounts as the uniform clean sand across a wide range of densities. These uniformly graded nonplastic silt test data provided no basis for arguing that these silts respond differently from uniform clean sand in its postliquefaction volumetric strain potential. Nonplastic silts with $D_r = 61\%$ to 67% in Fig. 5 reconsolidated similar amounts compared with Kizilirmak River sand with $D_r = 62\%$ to 69% and Toyoura sand with $D_r = 60\%$. The nonplastic silt results presented in Fig. 5 combined with those shown in Fig. 4 (as well as those shown in Figs. S1–S3) indicate uniformly graded nonplastic silty sand and uniformly graded nonplastic silt reconsolidated similar amounts as uniform clean sand if at similar relative densities under similar demands. Due to the limited amount of reconsolidation testing of silty soil relative to that of clean sand, additional testing of nonplastic silty soils is warranted.

Volumetric Strain Potential in Terms of Void Ratio

Initial void ratio (e_o) can be measured accurately in laboratory test specimens of nonplastic soils and soils with plasticity. As opposed to D_r , it can be used reliably to describe the state of soils with plastic fines. Given the intrinsic relation between e_o and D_r for soils of similar gradation, the void ratio can track with relative density for clean sand so its use as a unifying state index merits consideration (Fig. S4). In addition, void ratio is a fundamental state index related directly to soil compressibility and strength (Roscoe et al. 1958). Therefore, void ratio was evaluated for its potential to estimate the postliquefaction volumetric strain of soil.

Volumetric Strain Response of Clean Sand

The $\gamma_{\rm max}$ - ε_v data from 10 different uniform clean sands analyzed previously in terms of D_r were reinterpreted using e_o . A linear variation of e_o from 0.53 to 0.81 was observed as D_r reduced from about 90% to 30% for these sands, with e_o varying within a narrower range than D_r . A bin size of 0.05 for e_o was used to interpret the data because larger bin sizes tend to mask details and trends in the data. The standard error of the linear model estimate of ε_v as a function of e_o for an individual uniform clean sand ranged from 0.17% to 0.52%. Combining data sets increased standard error from 0.25% to 0.87%.

The $\gamma_{\rm max}$ - ε_v data for a representative void ratio bin $e_o=0.65-0.70$ are shown in Fig. 6(a) with a proposed bilinear model that will be described subsequently. Additional insights are gained when examining the data in terms of e_o . For example, the results of the Wu (2002) data of Monterey sand prepared to $D_r=50\%$ to 55% do not belong with the Ishihara and Yoshimine (1992) data of Fuji River sand prepared to $D_r=47\%$ [Fig. 3(a)]. However, when those two same data sets are evaluated in terms of e_o [Fig. 6 (a)], the Wu (2002) data have e_o ranging from 0.65 to 0.68 and the Ishihara and Yoshimine (1992) data have $e_o=0.67$, so the data sets are now in the same bin. This classification by e_o shows agreement between these two data sets with clear trends in the ε_v - $\gamma_{\rm max}$ relationships. Similar trends are observed in Fig. S5 for other e_o bins.

Volumetric Strain Response of Nonplastic Silty Sand

The nonplastic silty sand data discussed in terms of D_r were also reinterpreted using their e_o . Test results on nonplastic silty sand cover e_o values from 0.70 to 0.87, with representative data shown in $e_o = 0.75$ –0.80 bin as shown in Fig. 6(b). It was found that ε_v varies from 1.5% to 1.9% for $\gamma_{\rm max} = 5.0\%$ to 6.6% (except for one outlier at $\gamma_{\rm max} = 10.6\%$). Overall, the silty sand data agreed with the linear trend observed in the clean sand data shown in lighter color. Hence, data in Fig. 6(b) and the additional data in Fig. S5 indicate that the silty sand data and the clean sand data can be grouped and used together for the development of $\gamma_{\rm max}$ - ε_v models based on e_o .

All these data correspond to $\gamma_{\text{max}} \leq 8\%$, where no plateau was reached yet. Similar to what was observed in clean sands,

 e_o classifies silty sand slightly differently from D_r , i.e., data grouped together in a given D_r bin (Fig. 4), belong to different e_o bins [Fig. 6(b)]. However, regardless of how the data are classified, both D_r and e_o indicate that uniform nonplastic silty sand and uniform clean sand respond similarly. Moreover, the data in Fig. 6(b) vary within a narrow range of ε_v and $\gamma_{\rm max}$, which provides a measure of the dispersion of the silty sand data classified in terms of e_o . This dispersion is consistent with that observed in the larger clean sand data sets in Fig. 6(a). Despite the limited number of test results on nonplastic silty sands, these data show that higher e_o values are related to higher ε_v , and that bilinear models for $\gamma_{\rm max}$ - ε_v can fit both soils.

Volumetric Strain Response of Silt

The postliquefaction volumetric strain potential of nonplastic silt and low-plasticity silt can be examined in terms of e_o . As observed for the clean sand data, linear relationships between e_o and D_r were observed for silty soil where e_o varied from 0.60 to 1.26 for a change of D_r from 99% to 20%. Inspection of this trend confirmed that silt can exist naturally at higher void ratios than sand and that silty soil deposits with relatively high void ratios (i.e., $e_o > 0.80$) were likely to reconsolidate more than sand deposits subjected to similar levels of earthquake-induced $\gamma_{\rm max}$.

The uniform nonplastic silt data of Beyzaei (2017) were reevaluated using e_o . Most of the silt data in this study were in the e_o range from 0.70 to 0.90. Fig. 7(a) presents representative data in the $e_o=0.70$ –0.75 bin where ε_v increased linearly from 1.3% to 1.7% as $\gamma_{\rm max}$ increased from 4.8% to 6.7%. This trend was consistent with that observed in the uniform clean sand data. Figs. 5 and 7(a) show that e_o classified the nonplastic silt data differently from D_r . For example, the Wu (2002) data with $e_o=0.70$ –0.74 correspond to $D_r=40\%$ –50% and 60%–70%, whereas the Beyzaei (2017) silt data with $e_o=0.73$ –0.74 correspond to $D_r=80\%$ –90%. Similar to nonplastic silty sands, the nonplastic silt in this study's database were sheared to $\gamma_{\rm max}\leq 8\%$ where no plateau developed yet. It was assumed the plateau of constant ε_v develops at $\gamma_{\rm max}\geq 8\%$ as observed in the clean sands.

Some reconsolidation testing was also available on low-plasticity clayey silt with $0 < PI \le 12$. Although low plasticity clayey silty soil can undergo cyclic mobility (e.g., Bray and Sancio 2006),

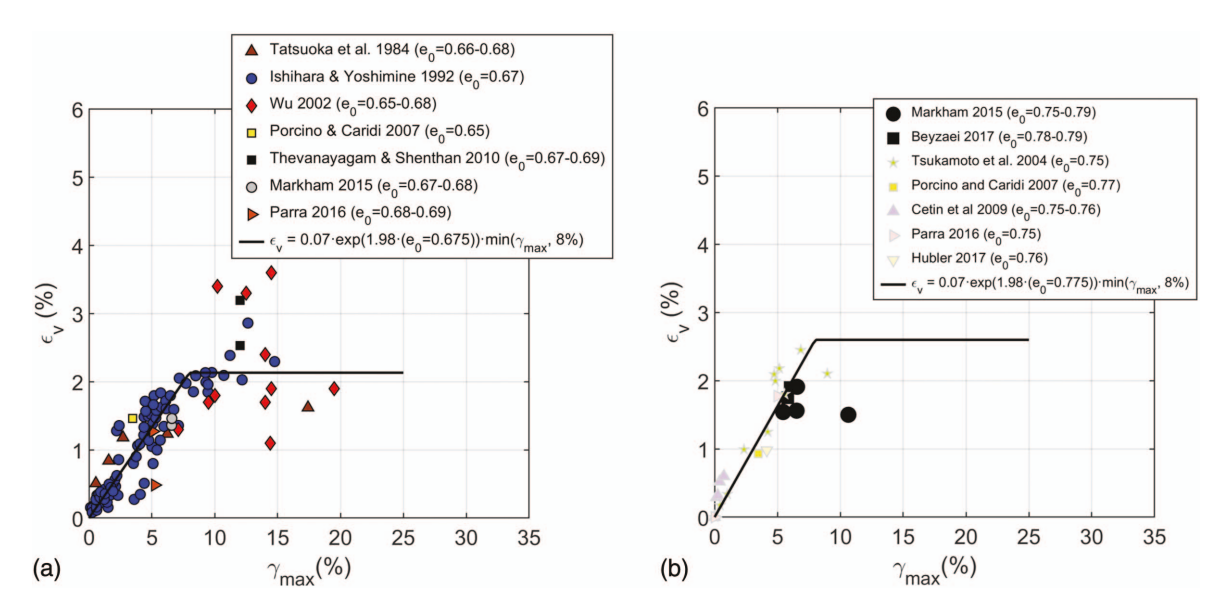


Fig. 6. (Color) Data for ε_v - $\gamma_{\rm max}$ in terms of void ratio for (a) clean uniform sand, $e_o = 0.65$ -0.70; and (b) silty sand, $e_o = 0.75$ -0.80.

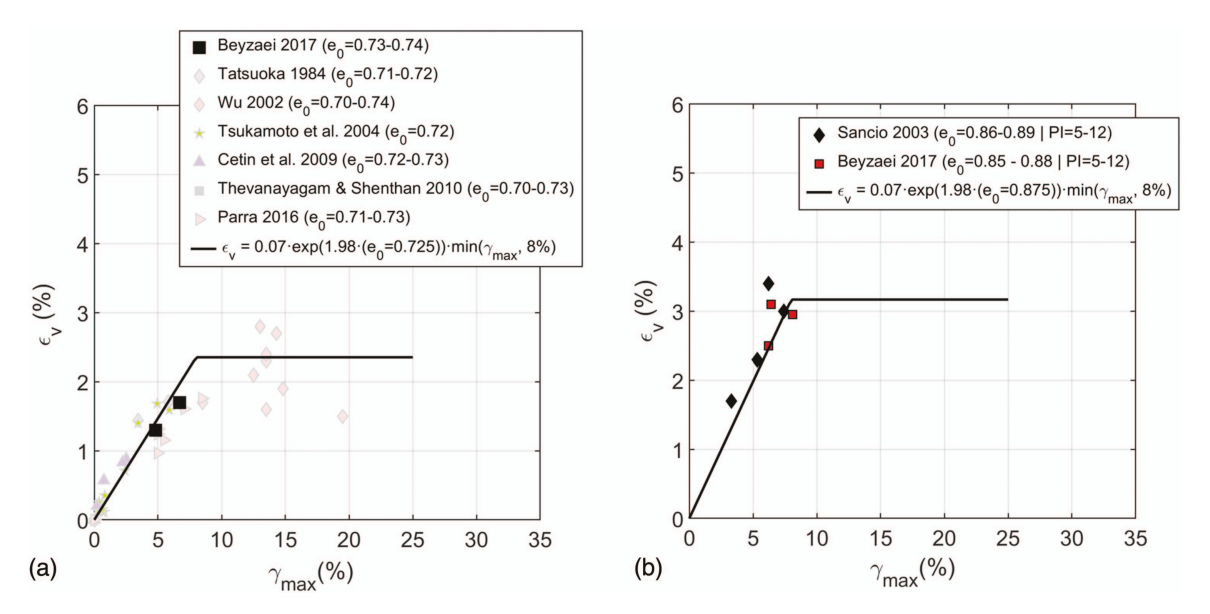


Fig. 7. (Color) Data for ε_v - $\gamma_{\rm max}$ data in terms of void ratio for (a) nonplastic uniform silt, $e_o = 0.70$ –0.75; and (b) low-plasticity uniform silt, $e_o = 0.85$ –0.90.

the addition of clay minerals can modify the cyclic response of a silt by limiting excess pore-water pressure generation and dissipating relatively more energy in each load cycle (Idriss and Boulanger 2008). As part of this study, reconsolidation of two low-plasticity silty soils from Adapazari and Christchurch (Sancio 2003; Beyzaei 2017, respectively) was analyzed using e_o as the independent variable. Low-plasticity silt postliquefaction volumetric strain data with e_o as the independent variable are presented in Fig. 7(b). The low-plasticity silts $\gamma_{\rm max}\text{-}\varepsilon_v$ data along with the same $e_o\text{-}{\rm dependent}$ bilinear model formulation employed for clean sand, nonplastic silty sand, and nonplastic silt show that a linear trend between ε_v and $\gamma_{\rm max}$ existed for PI \leq 12 silts up to $\gamma_{\rm max}=$ 8%, after which a ε_v plateau was apparent. Although there were differences in grain size and plasticity, the e_o -based classification of ε_v versus $\gamma_{\rm max}$ data captures the overall volumetric strain response of nonplastic soils and low-plasticity silts of uniform gradation with a single bilinear model formulation that will be described subsequently. Additional data on silts are shown in Fig. S6.

The empirical data on uniform clean sand, uniform silty sand, uniform nonplastic silt, and low-plasticity silt presented in this study indicate that e_o may be used to characterize the postliquefaction strain potential of these soils. In particular, e_o is advantageous relative to D_r for soils with high contents of fines because e_o is more widely and better known than D_r for silts. However, the data analyzed herein came from laboratory tests performed under known initial state and controlled boundary conditions. These two conditions are not typically met in the field, where the in situ e_o is difficult to estimate.

Volumetric Strain Response of Clayey Soil

Test data on plastic silts (PI > 12) and clays (as per USCS) indicated the excess pore-water pressure generated by cyclic loading can be as high as $r_u=0.7$ or 0.8 (Donahue 2007). Reconsolidation of the test specimens produced significant volumetric strains even though liquefaction was not triggered. Of the 52 clayey soil test results are available for this study, 30 of the tests by Bilge (2010) were sheared to $\gamma_{\rm max} \leq 2\%$, which does not fully inform ε_v relationships in terms of $\gamma_{\rm max}$. The clayey soil tested to $\gamma_{\rm max} > 2\%$ have $e_o=0.84$ to 1.7 and $13 \leq {\rm PI} \leq 53$. As shown in Fig. 8, no

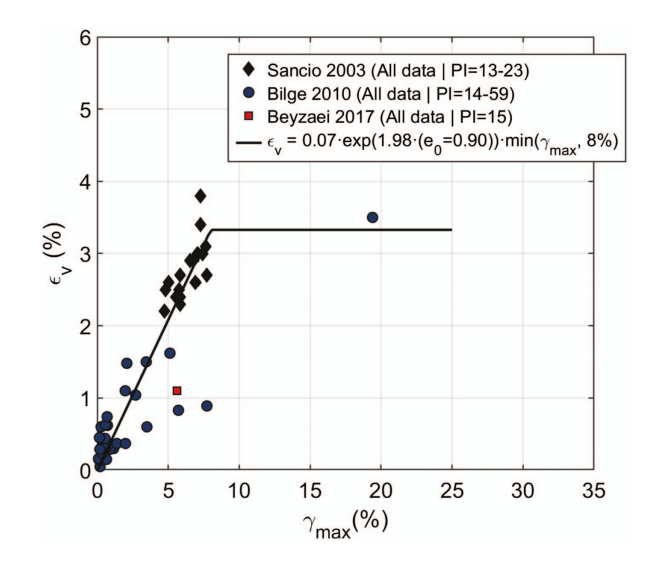


Fig. 8. (Color) Clayey soil ε_v - $\gamma_{\rm max}$ data in terms of void ratio.

appreciable differences in ε_v are observed as a function of e_o and PI.

It is possible to capture the response of all clayey soils in this study with a single bilinear model. Doing so is consistent with observations made from laboratory-based liquefaction tests studies where fine-grained clayey soils with PI > 12 develop similar stress-strain loops and similar pore-water pressure time histories. Data suggested that ε_v increases from zero to about 3.3% in a linear manner with increasing $\gamma_{\rm max}$ from zero to 8.0%, after which a plateau at $\varepsilon_v\approx 3.3\%$ was apparent. Additional postliquefaction reconsolidation testing of clayey soils is warranted to examine these trends further before developing findings for clayey soils.

Volumetric Strain Potential in Terms of the State Parameter

The SSL parameters of two clean sands (Toyoura and Ottawa), six sands with $5\% < FC \le 12\%$ (Christchurch SP–ML), one silty sand

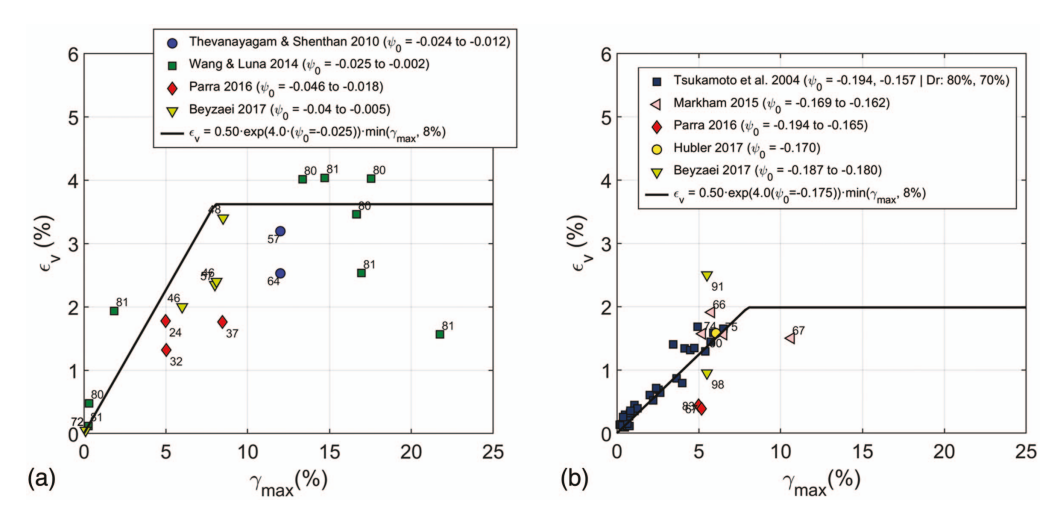


Fig. 9. (Color) Data for ε_v - $\gamma_{\rm max}$ in terms of state parameter: (a) $\psi_o = -0.05$ to 0.0; and (b) $\psi_o = -0.20$ to -0.15. Relative density (%) provided next to data point.

(Christchurch SM), and three silts (Christchurch ML) are available in the compiled database. Testing of these nonplastic soils produced 118 data points that were processed further to obtain their initial state parameter (ψ_o) as defined by Been and Jefferies (1985) as follows:

$$\psi_o = (e_o - e_c)|_{p_o'} \tag{1}$$

where e_o = current (in situ) void ratio at the current mean effective stress p_o' ; and e_c = void ratio at the critical state at the same p_o' . Hence, ψ_o characterizes the state of the soil by capturing simultaneously the influence of density and confining stress, as well as other factors such as grain size and shape and soil compressibility, using the SSL as a reference state. Jefferies and Been (2016) demonstrated that ψ_o provides a sound basis for describing and modeling soil response across a wide range of stress levels and loading conditions. Thus, from a mechanics perspective, it is desirable to develop models for γ_{max} - ε_v based on ψ_o .

Shuttle and Cunning (2007, 2008) showed that the limit between contractive and dilative response of cohesionless soils correspond to $\psi_o \approx -0.05$. Jefferies and Been (2016) suggested that the contractive/dilative response threshold of $\psi_o = -0.05$ is representative of simple shear conditions, whereas $\psi_o = -0.08$ is more representative of shear under triaxial conditions. Robertson (2016) and Mayne and Styler (2018) adopted $\psi_o = -0.05$ as the limit between contractive and dilative response when the CPT is used to estimate ψ_o in the field. The sandy and silty soils in this database also indicated that soils with $\psi_o < -0.05$ generated ε_v corresponding to dilative responses, which is consistent with these studies. The standard error of the linear estimate of ε_v as a function of ψ_o for an individual uniform clean sand was usually less than 0.53%. The standard error increased if data sets were combined, i.e., 0.36% to 0.98%.

Presentation of the volumetric strain versus maximum shear strain test data in terms of ψ_o for two representative bins of data are shown in Fig. 9. The relative density corresponding to each data point in the state parameter plots is also provided. In the $\psi_o=-0.05$ to 0.0 data range shown in Fig. 9(a), sands with D_r ranging from 24% to 64% and silts with D_r about 80% had similar ψ_o values of -0.024 to -0.009 (i.e., $\Delta\psi_o=0.015$). As illustrated in Fig. 9(b), test data on soils with $D_r=66\%$, 75%, and 90% (a difference of 24%) are represented by $\psi_o=-0.162$ to -0.170 $(\Delta\psi_o=0.008)$, indicating that some soils with different D_r values were at similar initial states in terms of ψ_o . Test specimens with

similar ψ_o exhibited similar ε_v when they were subjected to the same level of $\gamma_{\rm max}$. Similar observations in terms of stress–strain response curves and liquefaction susceptibility were reported by Been and Jefferies (1985). Although the state parameter is an informative index of the state of soil, its use in developing models is limited by the relatively few studies that provide the SSL (i.e., only about one-fifth of the studies in this database had SSL data). Thus, models using D_r and e_o are also developed because they have more data.

Laboratory-Based Models of Volumetric Strain Response of Soil

Regression Analysis of the γ_{max} - ε_{v} Database

Ishihara and Yoshimine (1992) developed their widely used chart containing FS_L - ε_v contours dependent on a clean sand's D_r to develop a procedure to estimate the postliquefaction settlement of natural sand deposits. Zhang et al. (2002) and Idriss and Boulanger (2008) developed relationships that approximated the Ishihara and Yoshimine (1992) curves to incorporate into their CPT-based procedures. However, these procedures do not clearly state the coupling among $\mathrm{FS}_L, \gamma_{\mathrm{max}},$ and $\varepsilon_v,$ and they do not measure the uncertainty of the postliquefaction ground settlement. Moreover, all procedures based on the Ishihara and Yoshimine (1992) curves are based on laboratory testing of just one clean sand. Cetin et al. (2009) developed a probabilistic standard penetration test (SPT)-based postliquefaction ground settlement procedure using results of a series of laboratory testing on clean sands, including Wu (2002); however, a probabilistic CPT-based procedure is also required in support of performance-based earthquake engineering. In this study, models relating ε_v , γ_{\max} , and FS_L were developed for a range of soil types using D_r , e_o , and ψ_o as independent variables and with quantification of the uncertainty of the estimate of volumetric strain.

The assembled database on uniform clean sand, uniform non-plastic silty sand, uniform nonplastic silt, and low-plasticity silt indicated ε_v increases linearly with increasing $\gamma_{\rm max}$ up to a $\gamma_{\rm max}$ threshold value $(\bar{\gamma})$ of about 7% to 9% for a given soil state, after which ε_v remains relatively constant with increasing shear strain. Accordingly, a bilinear model for ε_v versus $\gamma_{\rm max}$ was adopted with its break point at $\gamma_{\rm max}=\bar{\gamma}$ as follows:

$$\varepsilon_v = \theta \cdot \min(\gamma_{\text{max}}, \bar{\gamma}) \cdot e^{\varepsilon} \tag{2}$$

where θ = model parameters; and ε = error in the estimate. The function defined by Eq. (3) is minimized to determine the model parameters

$$f(\boldsymbol{\theta}, \boldsymbol{\varepsilon}_{v}, \boldsymbol{\gamma}_{\max}, \boldsymbol{\omega}) = \sum_{i} [\omega_{i} \cdot (\operatorname{Ln}(\varepsilon_{v_{i}}) - \operatorname{Ln}(\theta_{i} \cdot \min(\gamma_{\max i}, \bar{\gamma})))^{2} | \boldsymbol{\theta}]$$
(3)

where $f(\theta, \varepsilon_v, \gamma_{\max}, \omega)$ is a vector-valued function where vector ω contains a series of weights ϵ [0, 1] used in the nonlinear regression. The weights were assigned based on the quality, completeness, and extent of the test information. The primary test information are index properties, test type, liquefaction triggering criterion, CRR curves, γ_{\max} , and ε_v . Four classes of data were used in this database to represent the quality, completeness, and extent of the test information as summarized in Table 1 in a relative sense according to A with weight = 1; B with weight = 0.5; C with weight = 0.25; and D with weight = 0.

Cyclic triaxial testing, with its relatively larger test specimens and hence better resolution in volumetric strain measurements, was generally ranked higher than cyclic simple shear data; however, other variables were considered. The widely regarded data set from Ishihara and Yoshimine (1992), which was developed using simple shear tests with irregular loading, was assigned as Class A. Class B and Class C data sets had some noncritical characteristics about soil grain size or test conditions not reported. Additionally, Class C data sets had obvious outliers as defined subsequently. The data class criteria are summarized as follows:

- Class A: Cyclic triaxial test or irregularly loaded cyclic simple shear test. Soil grain-size characteristics, and test conditions were sufficiently described; information is available in tables or plots.
- Class B: Cyclic triaxial or cyclic simple shear test. Some noncritical characteristics about soil grain-size characteristics or test conditions were not reported; information is available in tables or plots.
- Class C: Cyclic triaxial or cyclic simple shear test. Some noncritical information about materials and test conditions was not reported; obvious outliers exist (i.e., an outlier is a data point in a data set that has more than a 2% volumetric strain deviation from its mean value).
- Class D: Not satisfying the criteria for Classes A, B, or C.

In examining the data, there was not a clear value of $\gamma_{\rm max}$ at which the ε_v plateau started; rather it ranged from 7% to 9%. Two break points (i.e., $\bar{\gamma}=8\%$ or 9%) in the bilinear regression models were evaluated to explore this issue. Using $\bar{\gamma}=8\%$ rendered slightly higher coefficient of determination (R^2) and slightly smaller standard deviations across the three state indexes discussed in this paper, and therefore, the proposed models in this study use $\bar{\gamma}=8\%$. Linear, quadratic, and exponential forms for θ were evaluated considering not only how well the data are fit but also considering that θ should allow the model to reproduce mechanistically sound responses over a wide range of densities. For example, data from Ishihara and Yoshimine (1992), Wu (2002), and Cetin et al. (2009) showed that ε_v increased at a higher rate as D_r decreased toward low D_r values. This trend in soil response needs to be captured by the chosen form of θ .

Relative Density γ_{max} - ε_v Model

It has been shown that uniform clean sand, gravel, nonplastic silty sand, and nonplastic silt can be categorized using D_r . After examining separately and observing similar responses, all these data were used in the regression analyses to develop a ε_v - $\gamma_{\rm max}$ model by setting the model parameter θ in Eq. (2) to be a function of D_r . Following the minimization defined by Eq. (3), a series of nonlinear regression analyses of the uniform nonplastic soil data were performed using different mathematical forms for θ , first over the entire data set and then over each individual D_r bin for each trial of θ until an efficient form was found. The resulting model to estimate ε_v (as a percentage) as function of $\gamma_{\rm max}$ (as a percentage) for a specified value of D_r (as a decimal) is

$$\varepsilon_v = 1.14 \cdot \exp(-2.0 \cdot D_r) \cdot \min(\gamma_{\text{max}}, 8\%) \cdot e^{\varepsilon}$$
 (4)

where ε = model residual. The form of this model is like that proposed by Yoshimine et al. (2006). The quantile-quantile distribution of residuals obtained from the proposed model was evaluated to select the appropriate scale for the standard deviation (σ). The proposed ε_v - $\gamma_{\rm max}$ model residuals are normally distributed and unbiased with zero mean and $\sigma=0.62$ in natural log units.

The proposed bilinear model and the $\pm 1\sigma$ range for $D_r = 70\%$ –80% are illustrated in Fig. 10(a), where the observed data trends are captured well. The proposed model contours for D_r values from 30% to 90% are shown in Fig. 10(b), along with the Ishihara and Yoshimine (1992) clean sand curves for comparison.

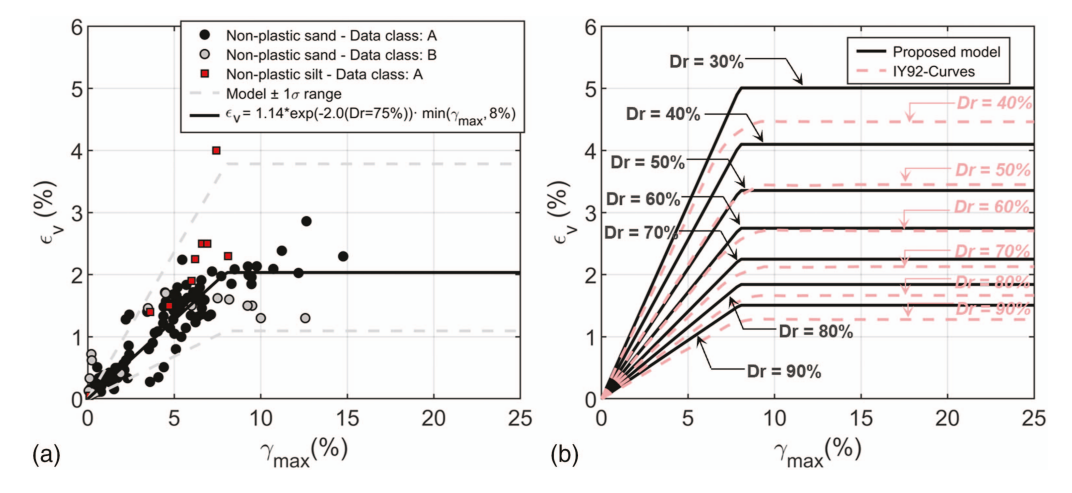


Fig. 10. (Color) Nonplastic uniform soil ε_v - $\gamma_{\rm max}$ proposed model in terms relative density: (a) $D_r = 70\%$ -80%; and (b) model contours.

Table 2. Coefficient of determination (R^2) of the proposed models

$\gamma_{ ext{max}}$ - $arepsilon_v$ model								FS_L - γ_{max} model					
Relative density, D_r			Void ratio, e_o		State parameter, ψ_o		Relative density, D_r			Void ratio, e_o			
D_r	Proposed model R^2	Y06 model ^a R ²	e_o	Proposed model R ²	ψ_o	Proposed model R ²	D_r	Proposed model R^2	Y06 model ^a R ²	e_o	Proposed model R ²		
40–50	0.63	0.56	0.85-0.90	0.67	0.0 to 0.05	0.27	40-50	0.47	0.41	0.80-0.85	0.27		
50-60	0.54	0.54	0.80 - 0.85	0.79	-0.05 to 0.0	0.46	50-60	_	_	0.75 - 0.80	0.79		
60-70	0.58	0.57	0.75 - 0.80	0.57	-0.10 to -0.05	0.37	60-70	0.79	0.71	0.70 - 0.75	0.22		
70-80	0.55	0.49	0.70 - 0.75	0.54	-0.15 to -0.10	0.76	70-80	0.63	0.40	0.65 - 0.70	0.69		
80-90	0.34	0.22	0.65 - 0.70	0.59	-0.20 to -0.15	0.74	80-90	0.44	0.62	0.60 - 0.65	0.14		
90–100	0.53	0.43	0.60-0.65	0.43	-0.25 to -0.20	0.48	90-100	0.58	0.62	0.55-0.60	0.49		

^aThe Yoshimine et al. (2006) (Y06) bilinear model is a parametrization of the Ishihara and Yoshimine (1992) curves.

The results of the regression analyses using the enlarged database indicate ε_v should vary within a slightly narrower range than envisioned previously. For example, the proposed model estimates a maximum $\varepsilon_v \approx 4.1\%$ at large shear strain for $D_r = 40\%$, which is lower than the Ishihara and Yoshimine (1992) estimate of 4.5%. At a high $D_r = 90\%$, the proposed model calculates a maximum $\varepsilon_v \approx 1.5\%$, which is slightly higher than the Ishihara and Yoshimine (1992) estimate of 1.3%. At $\gamma_{\rm max}$ smaller than 8%, there are also differences in the slope of the linear part of the model, particularly at low densities ($D_r \leq 40\%$) and high densities ($D_r \geq 70\%$). These observed changes are important for CPT applications where the soil profile is subdivided in several layers with different D_r .

The relative performance of the strain potential models is presented in terms of the coefficient of determination, R^2 because it is a measure of how well a model explains the data in each D_r bin and enables comparison with the Yoshimine et al. (2006) model. Ishihara and Yoshimine (1992) did not provide a functional form to their curves, so the R^2 of this study's model is compared with the Yoshimine et al. (2006) approximation of their curves. Table 2 summarizes the R^2 values for each D_r bin.

The R^2 values of the proposed model are slightly better than those of the Yoshimine et al. (2006) model. The higher R^2 values achieved with the new model indicate that it is better constrained by new test data at low and high relative densities. Eq. (4) is proposed

for uniform nonplastic soils, i.e., gravel, clean sand, nonplastic silty sand, and nonplastic silt. There is not a significant difference in estimating ε_v due to soil type if D_r is used to characterize the state of these uniformly graded soils using the Japanese $e_{\rm max}$ and $e_{\rm min}$ standards [JIS A 1224:2000 (Japanese Geotechnical Society 2000)].

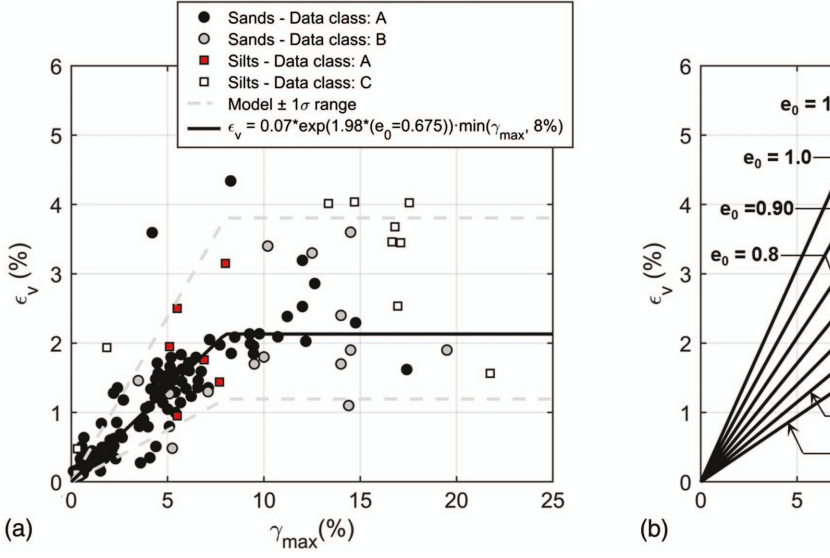
Void Ratio γ_{max} - ε_{v} Model

Similar to the D_r -based model, linear, quadratic, and exponential forms of the model were evaluated to develop a γ_{\max} - ε_v model in terms of void ratio. The resulting model to estimate ε_v (as a percentage) as function of γ_{\max} (as a percentage) for a specified value of e_o (as a decimal) is

$$\varepsilon_v = 0.07 \cdot \exp(1.98 \cdot e_o) \cdot \min(\gamma_{\text{max}}, 8\%) \cdot e^{\varepsilon} \tag{5}$$

The model residuals are zero-mean normally distributed with $\sigma=0.58$ in natural log units.

Fig. 11(a) shows the proposed model for $e_o=0.65$ to 0.70 where mostly sand data are included. The proposed model is also compared with silty sand data in the $e_o=0.75$ –0.80 range in Fig. 6(b) and with nonplastic silt and low-plasticity silt data in the $e_o=0.70$ –0.75 and $e_o=0.85$ –0.90 bins, respectively, in Fig. 7.



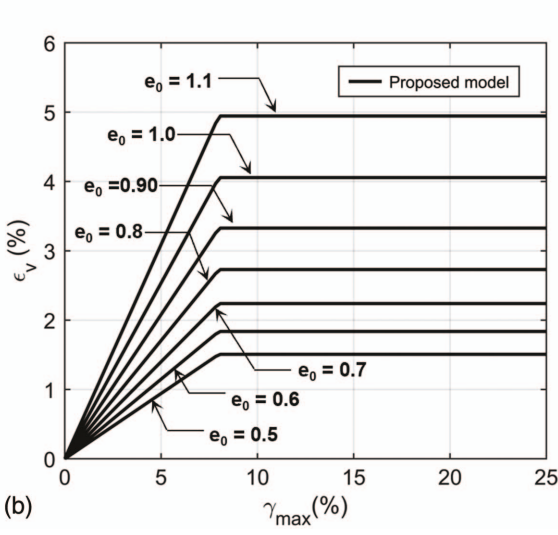


Fig. 11. (Color) Nonplastic uniform and low-plasticity uniform soil ε_v - $\gamma_{\rm max}$ proposed model in terms of void ratio: (a) $e_o=0.65$ -0.70; and (b) model contours.

The proposed e_o -based model captures reasonably well the ε_v - $\gamma_{\rm max}$ data over a range of materials and states. The ε_v - $\gamma_{\rm max}$ contours for e_o values between 0.5 and 1.1 are shown in Fig. 11(b), where ε_v varies from around 1.5% to a 5% over this range of e_o . Table 2 presents the R^2 values of the proposed model for each e_o bin. Overall, the e_o -based model performes satisfactorily; however, it may sometimes not capture well the clean sand response, especially at high e_o and large $\gamma_{\rm max}$ (Fig. S9). Therefore, it should only be used when ψ_o or D_r are not known reliably. Eq. (5) is proposed to be used primarily with uniform nonplastic fine soils and uniform low-plasticity soils.

State Parameter γ_{max} - ε_{v} Model

Test data presented in Fig. 9 showed the state parameter has potential for categorizing the volumetric strain of uniform clean sand, silty sand, and nonplastic silt in a unified manner. Although the state parameter shows promise, there are fewer data available because the SSL was not determined in most of the testing programs. Thus, the $\gamma_{\rm max}$ - ε_v model for ψ_o developed in this study is considered preliminary. Additionally, there is greater uncertainty in estimating ψ_o in situ relative to D_r and e_o . The model developed to estimate ε_v (as a percentage) as function of $\gamma_{\rm max}$ (as a percentage) for a specified value of ψ_o (as a decimal) is

$$\varepsilon_v = 0.50 \cdot \exp(4.0 \cdot \psi_o) \cdot \min(\gamma_{\text{max}}, 8\%) \cdot e^{\varepsilon} \tag{6}$$

The model residuals are zero-mean normally distributed with $\sigma=0.56$ in natural log units. Initially, the dilative/contractive threshold of $\psi_o=-0.05$ was included in the regression analysis because the response of soil changed significantly across this threshold. The results from various regression analyses were compared first over the entire database, next using the database divided in two groups one with $\psi_o<-0.05$ and a second one with $\psi_o\geq-0.05$, and finally over each individual ψ_o bin. However, the trends in the data and the scatter were not explained better by including the threshold $\psi_o=-0.05$ in the regression. Hence, the model was simplified to the version presented in Eq. (6).

The proposed bilinear model and the $\pm 1\sigma$ range for $\psi_o = -0.15$ to -0.10 are illustrated in Fig. 12(a), where the observed data trends are captured well. The proposed model contours for ψ_o values from -0.25 to 0.05 are shown in Fig. 12(b).

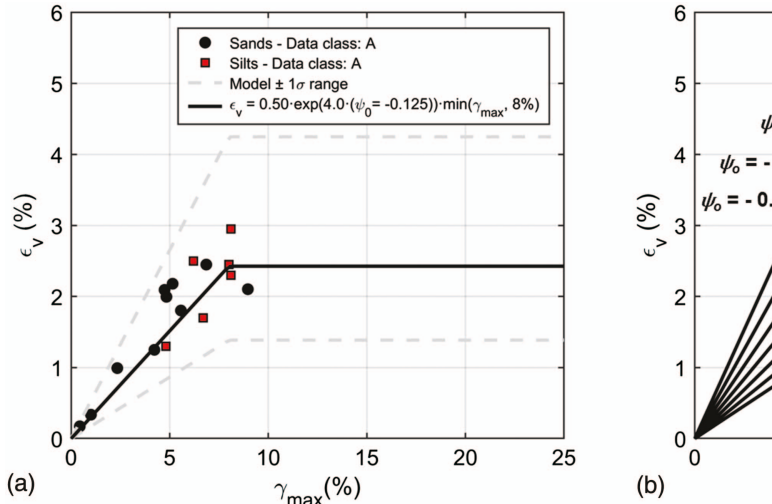
Like the D_r -based and e_o -based models, $\varepsilon_{v_{\rm max}}$ varies within a range of about 1.5% to about 5% for the range of test data available. Table 2 lists the R^2 values of the proposed model for each ψ_o bin. Overall, the ψ_o -based model performed reasonably well considering the limitations of the data. Importantly, the R^2 values were highest for ψ_o between -0.20 and -0.10, which corresponds to the range of ψ_o encountered in many natural soil deposits. Eq. (6) may be used with uniform nonplastic soils, although caution is warranted because the database used to develop this model is limited.

Normalizing ψ_o by the slope of the steady-state line λ_{10} provides a measure of potential strength loss because ψ_o/λ_{10} represents the ratio of the current mean effective stress (p'_o) to the mean effective stress at the critical state at the same void ratio (p'_c) and $p'_o/p'_c = \exp(-\psi_o/\lambda_{10})$. The normalized state parameter ψ_o/λ_{10} captures an undrained load path appropriate for liquefaction, so there is merit in developing an alternative $\gamma_{\rm max}$ - ε_v model based on ψ_o/λ_{10} . In the database, λ_{10} ranged from 0.025 to 0.129 (typical of clean sand to silty sand) with much of the volumetric strain data in the ψ_o/λ_{10} range of -6.0 to 2.0. Different bin widths were investigated, and a bin width of 1.25 grouped the data evenly with $\psi_o/\lambda_{10}=-1.25$ and 0.0 corresponding approximately to $\psi_o=-0.05$ and 0.0, respectively. The proposed bilinear model defined in Eq. (7) and shown in Fig. 13 has zero-mean natural log residuals with $\sigma=0.46$ in natural log units

$$\varepsilon_v = 0.48 \cdot \exp(0.21 \cdot (\psi_o/\lambda_{10})) \cdot \min(\gamma_{\text{max}}, 8\%) \cdot e^{\varepsilon}$$
 (7)

Maximum Shear Strain Potential of Liquefied Soil

Nagase and Ishihara (1988) assessed the results of many consistently prepared cyclic simple shear tests subjected to irregular and sinusoidal cyclic loads to identify that initial liquefaction (FS_L = 1.0) occurred at a single-amplitude shear strain ($\gamma_{\rm cyc,SA}$) between 3% and 3.5%. Later, Ishihara and Yoshimine (1992) recognized that 3.5% $\gamma_{\rm cyc,SA}$ is a convenient threshold because it is consistent with the 5% double-amplitude axial strain ($\gamma_{\rm cyc,DA}$) criterion used in cyclic triaxial tests. Moreover, they identified an inverse relationship between FS_L and $\gamma_{\rm max}$. Although other researchers have suggested slightly different strain criteria for defining the onset of liquefaction [e.g., Wu et al. (2004) adopted 3% $\gamma_{\rm cyc,SA}$ based on their cyclic simple shear tests], $\gamma_{\rm cyc,SA} = 3.5\%$ was adopted in this



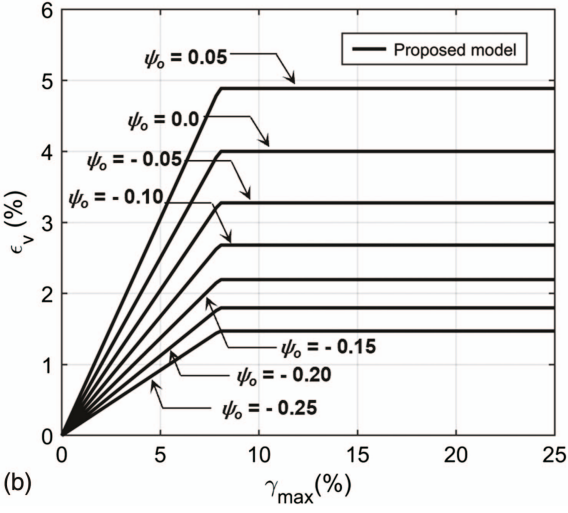


Fig. 12. (Color) Nonplastic uniform soil ε_v - $\gamma_{\rm max}$ proposed model in terms of state parameter: (a) $\psi_o = -0.15$ to -0.10; and (b) model contours.

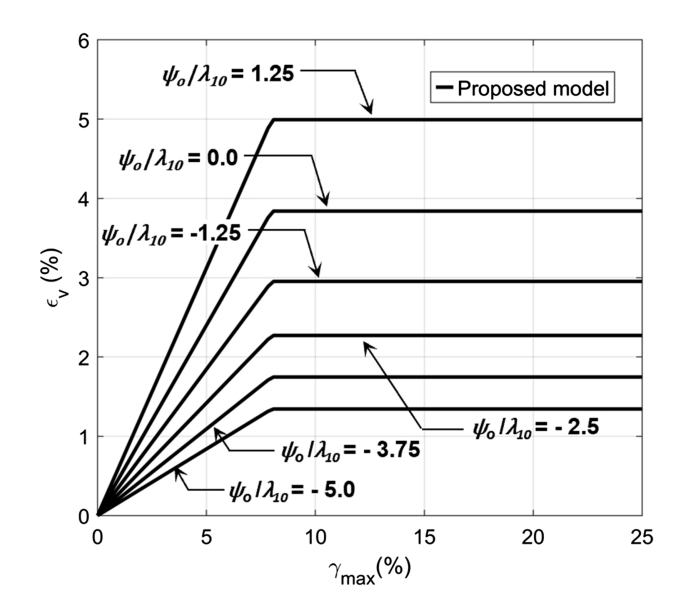


Fig. 13. Nonplastic uniform soil ε_v - $\gamma_{\rm max}$ proposed model in terms of the normalized state parameter ψ_o/λ_{10} .

study to be consistent with the Ishihara and Yoshimine (1992) database.

In cyclic simple shear tests, the CSR corresponding to $\gamma_{\rm cyc,SA} \approx 3.5\%$ is termed the cyclic resistance ratio. The locus of several CRR points corresponding to different equivalent load cycle values (N_c) is called the CRR curve, and $N_c=15$ represents the equivalent number of load cycles of a reference earthquake moment magnitude of 7.5 (Seed et al. 1975; Seed 1979). Different cyclic resistance curves would be obtained if different $\gamma_{\rm cyc,SA}$ values were selected. For $N_c=15$, the CRR at $\gamma_{\rm cyc,SA}=3.5\%({\rm CRR}_{3.5\%})$ is linked to FS $_L=1.0$, whereas the CSR at other levels of shear strain will correspond to FS $_L={\rm CRR}_{3.5\%}/{\rm CSR}$. Therefore, CSRs generated at different $\gamma_{\rm max}$ (e.g., 1%, 3.5%, 7%) can be used to generate different pairs of FS $_L$ and $\gamma_{\rm max}$.

From the Fuji River clean sand data set prepared at $D_r = 47\%$, 73%, and 93%, 164 FS_L- $\gamma_{\rm max}$ data points were available. Wu (2002), Sancio (2003), Markham (2015), and Beyzaei (2017) performed liquefaction resistance tests from which information about CRR versus N_c for $\gamma_{\rm cyc,SA} = 3.5\%$ and CSR for $\gamma_{\rm cyc,SA}$ levels other than 3.5% could be retrieved. This information was re-interpreted following the Ishihara and Yoshimine (1992) procedure described previously to generate 62 additional FS_L- $\gamma_{\rm max}$ data points corresponding to uniform clean sands, uniform nonplastic silty sands, and uniform nonplastic silts for D_r from 45% to 92%.

Additionally, test results from Tsukamoto et al. (2004) were reevaluated and filtered to produce 62 FS_L- $\gamma_{\rm max}$ data points corresponding to Toyoura sand and Kobe gravel prepared at $D_r = 60\%$ to 90%. Lastly, 11 FS_L- $\gamma_{\rm max}$ data points corresponding to Kobe silty sands prepared at $D_r = 72\%$ and 84% from Toriihara et al. (2000) were obtained. Thus, 299 FS_L- $\gamma_{\rm max}$ data points covering a wide range of relative densities and nonplastic uniform soil types were available for this study, as noted in Table 1. The new FS_L- $\gamma_{\rm max}$ data set is larger than that developed by Ishihara and Yoshimine (1992), and it includes a wide range of soil types as opposed to one clean sand.

The proposed models for $\gamma_{\rm max}$ as function of FS_L were developed primarily to capture the trends observed in the enlarged database and the data class defined previously. However, the models were not only driven by test data. Two physical constraints were introduced so physically meaningful estimates of $\gamma_{\rm max}$ were

obtained. First, the model must be consistent with the strain level corresponding to $FS_L = 1.0$ used during the laboratory data reduction; thus, the model was forced to pass through the point $(\gamma_{\rm max}, FS_L) = (3.5\%, 1.0)$ regardless of the soil's state. Second, the model assumes $\gamma_{\rm max} = 0$ if $FS_L \ge 2.0$ based on the findings of Dobry and Ladd (1980), who showed clean sand sheared to $\gamma_{\rm max} \le 0.01\%$ (volumetric threshold strain) developed negligible excess pore-water pressure $(r_u \approx 0)$. This is also supported by Marcuson et al. (1990), who showed r_u is on average less than 0.1 if $FS_L \ge 2.0$, and by Nagase and Ishihara (1988), who showed negligible ε_v values are generated (which implies negligible $\gamma_{\rm max}$), if $r_u < 0.3$. The test results in this database also indicate $\gamma_{\rm max}$ approaches zero as FS_L approaches 2.0.

Relative Density FS_L-\(\gamma_{\text{max}}\) Model

Examination of the enlarged database indicates that it is appropriate to adjust the trends presented by Ishihara and Yoshimine (1992) to fit the larger data set better. Initial regressions indicated that a hyperbolic relationship captures the FS_L - γ_{max} data trends well. Thus, hyperbolic forms with different degrees of freedom, including the two constraints discussed previously, were investigated. To avoid having curves at different D_r values cross when relating FS_L and strain potential, as will be discussed subsequently, the model required a slightly different curvature once $FS_L = 1.0$ was crossed; this is particularly important at high D_r . The nonlinear weighted regression resulted in a hyperbolic model that depends on one parameter (A) that is a function of D_r (as a decimal) as follows:

$$\gamma_{\text{max}} = 3.5 \cdot \left[\frac{2^A - FS_L^A}{2^A - 1} \right] \cdot e^{\varepsilon}$$

$$\gamma_{\text{max}} = 0 \quad \text{for } FS_L \ge 2.0$$
(8)

where

$$A = \begin{cases} -2.8 \cdot D_r^2 + 10.2 \cdot D_r - 9.8; & \text{FS}_L \ge 1.0 \\ -275 \cdot \exp(-6.6 \cdot D_r); & \text{FS}_L < 1.0 \end{cases}$$

The model residuals (ε) are zero-mean normally distributed with $\sigma=0.88$ in natural log units. The residuals of the model were analyzed using the same approach as the residuals of the ε_v - $\gamma_{\rm max}$ models. The quantile-quantile evaluation of residuals supports using natural log residuals. The obtained R^2 values of the proposed model for each D_r bin are listed in Table 2.

The proposed model with FS_L - γ_{max} data plotted for two D_r bins is presented in Fig. 14 with the Yoshimine et al. (2006) model for comparison (additional D_r bins are shown in Fig. S11). Significant scatter exists in the data, especially among data from different sources. For sand at looser states [Fig. 14(a)], the additional test data and the Ishihara and Yoshimine (1992) data show similar scatter with the proposed model deviating slightly from the Yoshimine et al. (2006) model. Conversely, the Tsukamoto et al. (2004) data and the additional data from this study for denser soils shown in Fig. 14(b) indicate γ_{max} reduces more than what is implied by the Ishihara and Yoshimine (1992) data when FS_L exceeded 1.0.

The proposed model exhibits stronger curvature than the existing relationship for dense soil. For $D_r=80\%$ –90%, the proposed model estimates larger $\gamma_{\rm max}$ than Yoshimine et al. (2006) at low FS_L (e.g., the proposed model estimates $\gamma_{\rm max}\approx 8.2\%$ for FS_L = 0.6, whereas the other model estimates $\gamma_{\rm max}\approx 7\%$). Conversely, at FS_L \geq 1.0 the proposed model estimates smaller $\gamma_{\rm max}$ than the Yoshimine et al. (2006) model. The proposed model provides improved estimates of $\gamma_{\rm max}$ at high D_r and high FS_L.

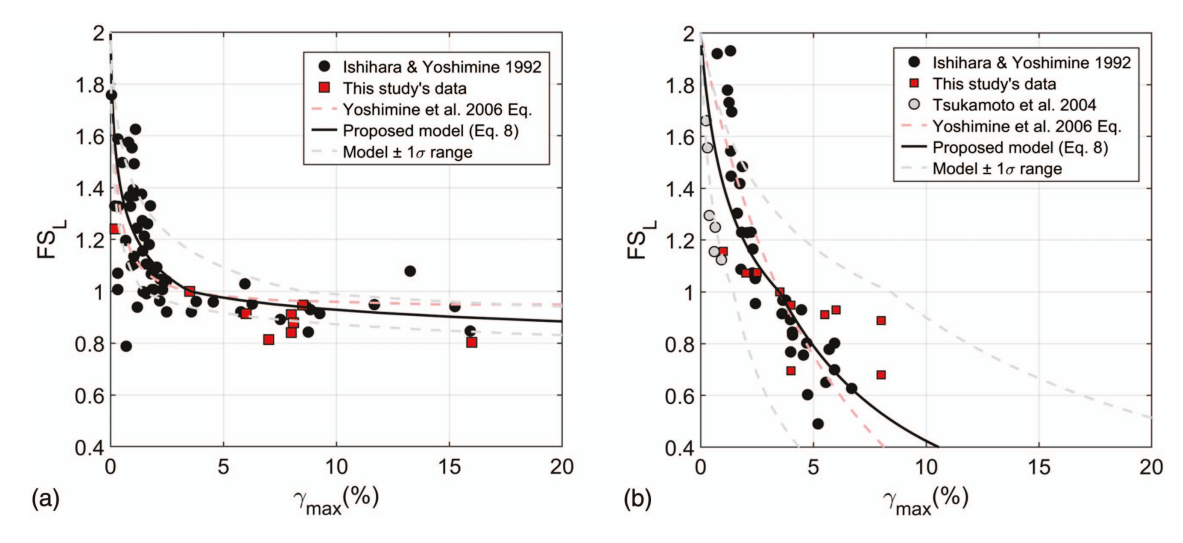


Fig. 14. (Color) Data for γ_{max} -FS_L and proposed model in terms relative density: (a) $D_r = 40\%$ -50%; and (b) $D_r = 90\%$ -100%.

The proposed model's fit for other D_r bins can be examined in the Supplemental Materials. Eq. (8) can be used in conjunction with Eq. (4) to estimate $\gamma_{\rm max}$ and ε_v for uniform nonplastic soil.

Void Ratio FS_L-γ_{max} Model

The FS_L- $\gamma_{\rm max}$ data can also be evaluated in terms of e_o , with $e_o = 0.54$ to 0.99. A representative e_o bin is shown in Fig. 15 along with the proposed model of Eq. (9) (additional e_o bins are shown in Fig. S12). Similar to the observations from the D_r categorization, significant scatter is observed. Aside from some minor differences, the trends observed using D_r are maintained in the e_o model. For instance, $\gamma_{\rm max}$ increases rapidly once FS_L < 1.0 at high void ratios (i.e., $e_o > 0.70$) in Fig. 15. Following the approach discussed previously, the FS_L- $\gamma_{\rm max}$ data are regressed using a hyperbolic model with two constraints with a change in curvature at FS_L = 1.0. The model parameter (*B*) is set to be a function of e_o (as a decimal) as presented in Eq. (9)

$$\gamma_{\text{max}} = 3.5 \cdot \left[\frac{2^B - \text{FS}_L^B}{2^B - 1} \right] \cdot e^{\varepsilon} \tag{9}$$

$$\gamma_{\text{max}} = 0$$
 for $F_L \ge 2.0$

where

$$B = \begin{cases} -5.33 \cdot e_o^2 + 2.67 \cdot e_o - 2.4; & \text{FS}_L \ge 1.0 \\ -9 \cdot 10^{-3} \cdot \exp(8.1 \cdot e_o); & \text{FS}_L < 1.0 \end{cases}$$

The model residuals (ε) follow a zero-mean normal distribution with $\sigma=0.89$ in natural log units. The proposed model's fit for other e_o bins can be found in the Supplemental Materials. The obtained R^2 values of the proposed model for each e_o bin are listed in Table 2. Similar to the observation made during the development of the ε_v - $\gamma_{\rm max}$ model in terms of e_o , sand data at high e_o were not as well-captured by e_o . Eq. (9) can be used in conjunction with Eq. (5) to estimate $\gamma_{\rm max}$ and ε_v for uniform nonplastic soil.

Relation between Relative Density and the State Parameter

Currently, there are not enough FS_L - γ_{max} data available to develop a model using ψ_o . Instead, the current database allows the development and calibration of a relationship between D_r and ψ_o that

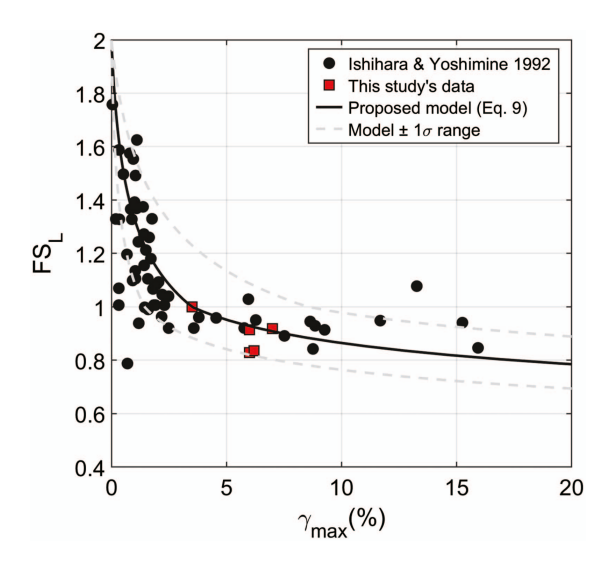


Fig. 15. (Color) Data for γ_{max} -FS_L and proposed model in terms of void ratio $e_o = 0.80$ –0.85.

delivers consistent estimates of ψ_o based on D_r . The calculation of ψ_o requires knowledge of the soil's SSL, and developing the SSL requires a series of specifically designed laboratory tests, which are not typically performed for most projects. However, the Bolton (1986) normalized dilatancy index equation can be used for a zero-dilation condition for sand to develop an estimate of relative density at the critical state ($D_{\rm rcs}$) (Mitchell and Soga 2005) as follows:

$$1 = D_{\rm rcs} \cdot \text{Ln}(\sigma'_{cr}/\sigma'_{c}) \tag{10}$$

where σ'_{cr} = soil's crushing stress; and σ'_{c} = effective normal/confining stress. This equation can be expanded to focus on e_{cs} as follows:

$$e_{\text{max}} - e_{cs} = (e_{\text{max}} - e_{\text{min}}) / \text{Ln}(\sigma'_{cr}/\sigma'_{c})$$
 (11)

Using the definition of D_r in conjunction with Eq. (10), ψ_o can be obtained as follows:

$$\psi_o = e_o - e_{cs} = \xi \cdot (e_{\text{max}} - e_{\text{min}})[1/\text{Ln}(\sigma'_{cr}/\sigma'_{c}) - D_{ro}]$$
 (12)

© ASCE 04022099-13 J. Geotech. Geoenviron. Eng.

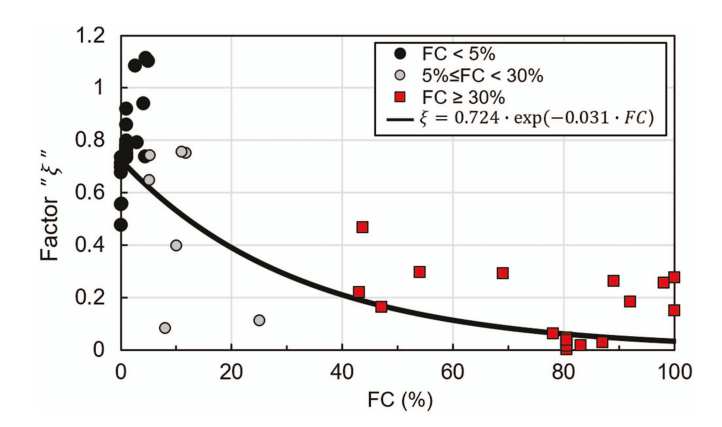


Fig. 16. (Color) Factor ξ in the state parameter relationship.

where D_{ro} = in situ D_r ; and coefficient ξ = adjustment factor that accounts for the aspects not captured by Eq. (12) and the variability of the individual relationships used to develop Eq. (12). For example, there is significant variability in estimation of $(e_{\text{max}}-e_{\text{min}})$, and Eq. (10) may not have the appropriate form for all soils. The ξ factor was determined through a calibration process using the collected testing database to account for the sources of error in the approximation of Eq. (12).

Examination of Eq. (12) using the test database showed the estimated ψ_o was not too sensitive to σ'_{cr} , so typical values estimated from Mitchell and Soga (2005) were used (i.e., 8,000 kPa for silt; 10,000 kPa for silty sand; and 20,000 kPa for clean sand). The average of the soil-dependent correlation of Cubrinovski and Ishihara (2002) was used to estimate ($e_{\rm max} - e_{\rm min}$). Fig. 16 displays the relationship of ξ with FC for about 60 test results, which is provided as follows:

$$\xi = 0.724 \cdot \exp(-0.031 \cdot FC)$$
 (13)

where FC is expressed in percent as an integer, and ξ has an average value of about 0.75 for uniform clean sand, 0.5 for uniform silty sand, and 0.1 for uniform silt. The small ξ for sandy silt and silt are due to ξ correcting for the factors described previously in addition to accounting for the application of the Bolton SSL equation to soils with high FC. The R^2 of Eq. (13) for ξ is 0.77. Site-specific measurements should be used to improve the reliability of Eq. (13) when possible because its current form is recommended for preliminary estimates.

Relating FS_L and Strain Potential

Ishihara and Yoshimine (1992) developed a widely used figure to estimate ε_v or $\gamma_{\rm max}$ versus ${\rm FS}_L$ as a function of a sand's D_r to estimate liquefaction-induced ground settlement or lateral spreading. Yoshimine et al. (2006) developed equations to capture the individual ${\rm FS}_L$ - $\gamma_{\rm max}$ and ε_v - $\gamma_{\rm max}$ relationships presented by Ishihara and Yoshimine (1992). However, the D_r contours drawn by Ishihara and Yoshimine (1992) in their ε_v versus ${\rm FS}_L$ figure cannot be obtained by combining the ${\rm FS}_L$ - $\gamma_{\rm max}$ and ε_v - $\gamma_{\rm max}$ equations presented by Yoshimine et al. (2006). For example, the Yoshimine et al. (2006) contours in their ε_v versus ${\rm FS}_L$ figure cross each other for $D_r \leq 60\%$ when ${\rm FS}_L \geq 1.0$; whereas the D_r contours drawn by Ishihara and Yoshimine (1992) do not cross. The shape of their D_r -dependent ${\rm FS}_L$ - $\gamma_{\rm max}$ relationships when ${\rm FS}_L \geq 1.0$, especially for high D_r values, was the primary cause of the inconsistency that results when combining the Yoshimine et al. (2006) equations.

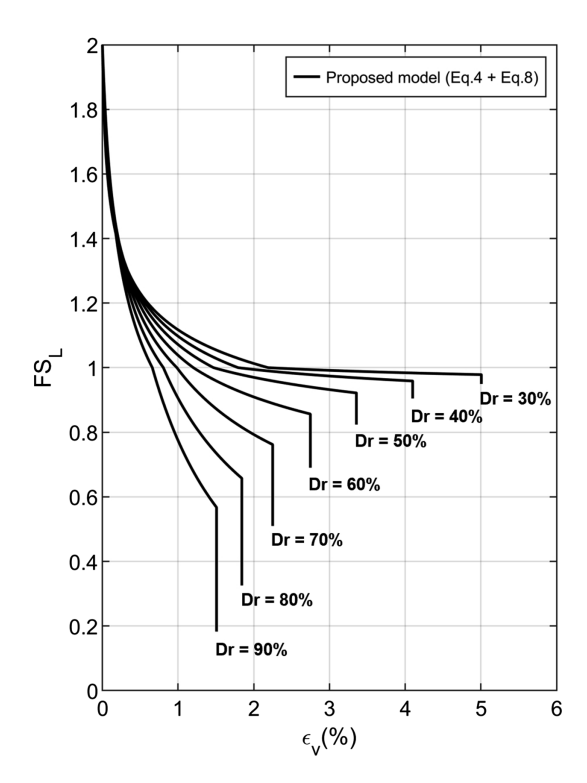


Fig. 17. Relationship between ε_v and FS_L in terms of D_r .

Using a model with slightly different curvatures once $FS_L = 1.0$ is crossed avoids this issue.

The models presented in this paper provide alternative estimates of ε_v and $\gamma_{\rm max}$ using three measures of the soil's state and FS_L as a proxy for the seismic demand. These models can be combined to estimate postliquefaction volumetric-induced free-field ground settlement in a consistent manner. The proposed models presented in Eqs. (8) and (9) avoid the issue described previously by using different curvatures when FS_L \geq 1.0 and FS_L < 1.0. The relationship between ε_v and FS_L as a function of D_r obtained from combining the FS_L- $\gamma_{\rm max}$ and ε_v - $\gamma_{\rm max}$ models in this study [i.e., Eqs. (4) and (8)] is shown in Fig. 17 as an example. The proposed equations provide D_r curves that do not cross.

Conclusion

The primary basis of several of the empirical methods used in engineering practice to estimate postliquefaction ground deformation is the laboratory data from one series of cyclic simple shear tests performed on one uniform clean sand reconstituted to three relative densities. An enlarged database containing 579 ε_v and 299 $\gamma_{\rm max}$ data points from cyclic tests on 10 uniform clean sands, 2 gravels, 3 silty sands, and 5 silts was developed to investigate if the trends of that one uniform sand data set are applicable to other uniform clean sands, uniform nonplastic silty sands, and uniform nonplastic silts. The enlarged database provides a basis to evaluate the effects of parameters such as particle size, PI, D_r , e_o , ψ_o , and FS_L, and to develop models to estimate liquefaction-induced maximum shear strain and postliquefaction volumetric strain. The proposed models include the uncertainty in the estimate.

The volumetric response of clean sand, nonplastic silty sand, and nonplastic silt in cyclic tests can be interpreted in a unified manner using the state parameter. However, the ψ_o -based model developed in this study is considered preliminary due to the relative

sparseness of the data available. It is hoped the ψ_o -based model will be refined as more steady-state test data become available. As an alternative to the state parameter, relative density can continue to be used to capture the volumetric response of uniform clean sand.

Moreover, a D_r -based model can provide insights on the volumetric response of uniform nonplastic silty sand and uniform nonplastic silt. Whereas the D_r -based model of Ishihara and Yoshimine (1992) was based on the results of just one sand, the proposed D_r -based model is based on a larger database of uniform nonplastic soils. For soils where D_r can be obtained reliably, D_r provides a practical means for categorizing postliquefaction reconsolidation data. In cases when neither ψ_o or D_r are available, void ratio can be used as the independent variable to characterize the liquefaction strain potential of nonplastic and low-plasticity silts. The database supports the use of bilinear models to capture the ε_v - $\gamma_{\rm max}$ relationship for uniform nonplastic soils using ψ_o , D_r , and e_o . The maximum volumetric strain is reached at a maximum shear strain of 8%. The results of the regression analyses using the enlarged database on nonplastic soil indicate ε_v should vary within a narrower range than estimated using the Ishihara and Yoshimine (1992) model.

The compiled database in conjunction with the concept of the volumetric threshold strain were used to propose new hyperbolic relationships for FS $_L$ versus $\gamma_{\rm max}$ with D_r as the primary independent variable for uniform nonplastic soils. A FS $_L$ - $\gamma_{\rm max}$ proposed model was also presented in terms of e_o . These new models implement equations that produce different curvature above and below FS $_L=1.0$ so consistent strain measures are obtained for different values of D_r and e_o . The current database does not contain enough data to develop a reliable FS $_L$ - $\gamma_{\rm max}$ model in terms of ψ_o . Instead, the available data were used to estimate ψ_o based on the soil's D_r . When combined, the proposed FS $_L$ - $\gamma_{\rm max}$ and ε_v - $\gamma_{\rm max}$ models developed in this study produced consistent D_r -dependent ε_v versus FS $_L$ contours.

Additional cyclic testing, especially of well graded clean sand, nonplastic silty sand, nonplastic silt, and low-plasticity silt, considering different states and confining stress are warranted to enhance the current database. Steady-state testing should be performed so the ψ_o -based model can be refined. Some of the testing should be performed before liquefaction is triggered and other testing continued well after liquefaction is triggered to strengthen the FS_L- $\gamma_{\rm max}$ models. Lastly, the proposed models can be used as the basis for developing field-based probabilistic liquefaction-induced volumetric strain and shear strain procedures for a wide range of soils. Limitations of the laboratory-based models (e.g., lack of SSL data) and differences of laboratory testing and field responses of soil (e.g., time under confinement effects for soil that does not liquefy) should be considered when applying the proposed laboratory models to field applications.

Data Availability Statement

All test data are available through the references provided in Table 1. Some or all data, models, or code that support the findings of this study are available from the corresponding author upon reasonable request.

Acknowledgments

This work was supported financially by the US National Science Foundation through Grant No. CMMI-1956248. Additional support was provided by the Faculty Chair in Earthquake Engineering

Excellence at UC Berkeley. The findings, opinions, and conclusions presented in this paper are those of the authors and do not necessarily reflect the views of the sponsoring bodies. The authors would like to thank Dr. K. Ishihara, who provided data and references on Fuji River sand and Japanese silty sands.

Supplemental Materials

Table S1 and Figs. S1–S12 are available online in the ASCE Library (www.ascelibrary.org).

References

- Been, K., and M. G. Jefferies. 1985. "A state parameter for sands." *Géotechnique* 35 (2): 99–112. https://doi.org/10.1680/geot.1985.35.2.99.
- Beyzaei, C. Z. 2017. "Fine-grained soil liquefaction effects in Christchurch, New Zealand." Ph.D. dissertation, Dept. of Civil and Environmental Engineering, Univ. of California.
- Beyzaei, C. Z., J. D. Bray, M. Cubrinovski, M. Riemer, and M. Stringer. 2018. "Laboratory-based characterization of shallow silty soils in southwest Christchurch." Soil Dyn. Earthquake Eng. 110 (Jan): 93–109. https://doi.org/10.1016/j.soildyn.2018.01.046.
- Bilge, H. T. 2010. "Cyclic volumetric and shear strain response of finegrained soils." Ph.D. dissertation, Dept. of Civil Engineering, Middle East Technical Univ.
- Bolton, M. D. 1986. "The strength and dilatancy of sands." *Géotechnique* 36 (1): 65–78. https://doi.org/10.1680/geot.1986.36.1.65.
- Boulanger, R. W., and K. Ziotopoulou. 2015. *PM4Sand (Ver 3)—A sand plasticity model for earthquake engineering applications*. Rep. No. UCD/CGM-15/01. Davis, CA: Univ. of California.
- Bray, J. D., R. W. Boulanger, M. Cubrinovski, K. Tokimatsu, S. L. Kramer, T. O'Rourke, E. Rathje, R. A. Green, P. Robertson, and C. S. Beyzaei. 2017. U.S.—New Zealand—Japan international workshop, liquefaction-induced ground movements effects. Rep. No. 2017/02. Berkeley, CA: Univ. of California.
- Bray, J. D., and R. B. Sancio. 2006. "Assessment of the liquefaction susceptibility of fine-grained soils." *J. Geotech. Geoenviron. Eng.* 132 (9): 1165–1177. https://doi.org/10.1061/(ASCE)1090-0241(2006) 132:9(1165).
- Cetin, K. O., H. T. Bilge, J. Wu, A. M. Kammerer, and R. B. Seed. 2009. "Probabilistic models for cyclic straining of saturated clean sands." *J. Geotech. Geoenviron. Eng.* 135 (3): 71–86. https://doi.org/10.1061/(ASCE)1090-0241(2009)135:3(371).
- Chin, R. 1987. "Volumetric strain characteristics of saturated sand under cyclic loadings." In Vol. 2 of *Proc.*, 9th Southeast Asian Geotechnical Conf., 7.81–7.90. Bangkok, Thailand: Southeast Asian Geotechnical Society.
- Cubrinovski, M. 2019. Some important considerations in the engineering assessment of soil liquefaction, 30–49. Wellington, New Zealand: New Zealand Geotechnical Society.
- Cubrinovski, M., and K. Ishihara. 2000. "Flow potential of sandy soils with different grain compositions." *Soils Found*. 40 (4): 103–119. https://doi.org/10.3208/sandf.40.4_103.
- Cubrinovski, M., and K. Ishihara. 2002. "Maximum and minimum void ratio characteristics of sands." *Soils Found.* 42 (6): 65–78. https://doi.org/10.3208/sandf.42.6_65.
- Dobry, R., and R. Ladd. 1980. "Discussion on "Soil liquefaction and cyclic mobility evaluation for level ground during earthquakes and liquefaction potential: Science versus practice." *J. Geotech. Eng. Div.* 106 (23): 720–724. https://doi.org/10.1061/AJGEB6.0000984.
- Donahue, J. L. 2007. "The liquefaction susceptibility, resistance, and response of silty and clayey soils." Ph.D. dissertation, Dept. of Civil and Environmental Engineering, Univ. of California.
- Duku, P. M., P. M. Stewart, D. H. Whang, and E. Yee. 2008. "Volumetric strains of clean sands subject to cyclic loads." *J. Geotech. Eng. Div.* 134 (8): 1073–1085. https://doi.org/10.1061/(ASCE)1090-0241(2008) 134:8(1073).

- Duncan, J. M., S. G. Wright, and T. L. Brandon. 2014. Soil strength and slope stability. New York: Wiley.
- Hubler, J. F. 2017. "Laboratory and in-situ assessment of liquefaction of gravelly soils." Ph.D. dissertation, Dept. of Civil and Environmental Engineering, Univ. of Michigan.
- Idriss, I., and R. Boulanger. 2008. *Soil liquefaction during earthquakes*. Oakland, CA: Earthquake Engineering Research Institute.
- Ishihara, K., and M. Yoshimine. 1992. "Evaluation of settlements in sand deposits following liquefaction during earthquakes." *Soils Found*. 32 (1): 173–188. https://doi.org/10.3208/sandf1972.32.173.
- Japanese Geotechnical Society. 2000. Test methods for minimum and maximum densities of sands. JIS A 1224:2000. Tokyo: Japanese Geotechnical Society.
- Jefferies, M., and K. Been. 2016. Soil liquefaction: A critical state approach. 2nd ed. New York: Taylor & Francis Group.
- Kazama, M. 2011. "Residual deformation property of liquefied soil and related phenomena." In Proc., 14th Asian Regional Conf. on Soil Mechanics and Geotechnical Engineering, 2522–2534. Hong Kong: Hong Kong Geotechnical Society.
- Lee, K. L., and A. Albaisa. 1974. "Earthquake induced settlements in saturated sands." J. Geotech. Eng. Div. 100 (4): 387–406. https://doi .org/10.1061/AJGEB6.0000034.
- Marcuson, W. F., M. E. Hynes, and A. G. Franklin. 1990. "Evaluation and use of residual strength in seismic safety analysis of embankment." *Earthquake Spectra* 6 (3): 529–572. https://doi.org/10.1193/1.1585586.
- Markham, C. S. 2015. "Response of liquefiable sites in the central business district of Christchurch, New Zealand." Ph.D. dissertation, Dept. of Civil and Environmental Engineering, Univ. of California.
- Markham, C. S., J. D. Bray, M. Cubrinovski, and M. Riemer. 2018. "Lique-faction resistance and steady-state characterization of shallow soils within the Christchurch central business district." J. Geotech. Geoenviron. Eng. 144 (6): 04018032. https://doi.org/10.1061/(ASCE)GT.1943-5606.0001823.
- Mayne, P. W., and M. Styler. 2018. "Soil liquefaction screening using CPT yield stress profiles." In *Proc.*, Geotechnical Earthquake Engineering Soil Dynamics 5, 605–616. Reston, VA: ASCE.
- Mijic, Z., J. D. Bray, M. F. Riemer, M. Cubrinovski, and S. D. Rees. 2021a. "Test method for minimum and maximum densities of small quantities of soil." *Soils Found*. 61 (2): 533–540. https://doi.org/10.1016/j.sandf.2020.12.003.
- Mijic, Z., J. D. Bray, M. F. Riemer, S. D. Rees, and M. Cubrinovski. 2021b. "Cyclic and monotonic simple shear testing of native Christchurch silty soil." *Soil Dyn. Earthquake Eng.* 148 (Sep): 106834. https://doi.org/10 .1016/j.soildyn.2021.106834.
- Mitchell, J., and K. Soga. 2005. Fundamentals of soil behavior. 3rd ed. New York: Wiley.
- Nagase, H., and K. Ishihara. 1988. "Liquefaction-induced compaction and settlement of sand during earthquakes." Soils Found. 28 (12): 65–76. https://doi.org/10.3208/sandf1972.28.65.
- Parra, A. M. 2016. "Ottawa F-65 sand characterization." Ph.D. dissertation, Dept. of Civil and Environmental Engineering, Univ. of California.
- Porcino, D., and G. Caridi. 2007. "Pre- and post-liquefaction response of sand in cyclic simple shear." In *Proc.*, ASCE Geo-Denver 2007. Reston, VA: ASCE.
- Robertson, P. K. 2016. "Cone penetration test (CPT)-based soil behaviour type (SBT) classification system—An update." *Can. Geotech. J.* 2016 (1): 1–18. https://doi.org/10.1139/cgj-2016-0044.
- Roscoe, K. H., A. N. Schofield, and C. P. Wroth. 1958. "On the yielding of soils." *Géotechnique* 8 (22): 22–53. https://doi.org/10.1680/geot .1958.8.1.22.
- Sancio, R. B. 2003. "Ground failure and building performance in Adapazari, Turkey." Ph.D. dissertation, Dept. of Civil and Environmental Engineering, Univ. of California.
- Seed, H. B. 1979. "Soil liquefaction and cyclic mobility evaluation for level ground during earthquakes." J. Geotech. Eng. Div. 105 (2): 201–255. https://doi.org/10.1061/AJGEB6.0000768.

- Seed, H. B., I. M. Idriss, F. Makdisi, and N. Barnerjee. 1975. Representation of irregular stress time histories by equivalent uniform stress series in liquefaction analyses. Oakland, CA: Earthquake Engineering Research Center.
- Sento, N., M. Kazama, R. Uzuoka, A. Matsuya, and M. Ishimaru. 2004. "Liquefaction-induced volumetric change during re-consolidation of sandy soil subjected to undrained cyclic loading histories." In *Proc.*, *Cycle Behaviour of Soil and Liquid Phenomena*, 199–207. New York: Taylor and Francis.
- Shamoto, Y., M. Sato, and J. Zhang. 1996. "Simplified estimation of earthquake-induced settlements in saturated sand deposits." Soils Found. 36 (9): 39–50. https://doi.org/10.3208/sandf.36.39.
- Shuttle, D. A., and J. Cunning. 2007. "Liquefaction potential of silts from CPTu." *Can. Geotech. J.* 45: 140–141. https://doi.org/10.1139/t06-086.
- Shuttle, D. A., and J. Cunning. 2008. "Reply to the discussion by Robertson on 'liquefaction potential of silts from CPTu." *Can. Geotech. J.* 45: 142–145. https://doi.org/10.1139/T07-119.
- Silver, M. L., and H. B. Seed. 1971. "Volume changes in sands during cyclic loading." J. Soil Mech. Found. Div. 97 (9): 1171–1182. https://doi.org/10.1061/JSFEAQ.0001658.
- Tatsuoka, F., T. Sasaki, and S. Yamada. 1984. "Settlement in saturated sand induced by cyclic undrained simple shear." In Vol. 3 of *Proc.*, 8th World Conf. on Earthquake Engineering, 398–405. Oakland, CA: Earthquake Engineering Research Institute.
- Thevanayagam, S., and J. Shenthan. 2010. "Cyclic pore pressure generation, dissipation and densification in granular mixes." *Int. J. Geotech. Earthquake Eng.* 2010 (Jan): 42–61. https://doi.org/10.4018/jgee.2010090803.
- Thevanayagam, S., T. Shenthan, S. Mohan, and J. Liang. 2002. "Undrained fragility of clean sands, silty sands, and sandy silts." *J. Geotech. Geoenviron. Eng.* 128 (10): 849–859. https://doi.org/10.1061/(ASCE)1090-0241(2002)128:10(849).
- Tokimatsu, K., and H. B. Seed. 1977. "Evaluation of settlement in sands due to earthquake shaking." *J. Geotech. Eng. Div.* 113 (8): 861–878. https://doi.org/10.1061/(ASCE)0733-9410(1987)113:8(861).
- Toriihara, M., Y. Yamada, I. Morimoto, and K. Ishihara. 2000. "The characteristics of settlement after liquefaction for sand containing fines." [In Japanese.] In Vol. 3 of *Proc.*, 35th Japan Conf. on Geotechnical Engineering, 1655–1656. Tokyo: Japanese Geotechnical Society.
- Tsukamoto, Y., K. Ishihara, and S. Sawada. 2004. "Settlement of silty sand deposits following liquefaction during earthquakes." *Soils Found*. 44 (6): 135–148. https://doi.org/10.3208/sandf.44.5_135.
- Wang, S., and R. Luna. 2014. "Compressibility characteristics of low-plasticity silt before and after liquefaction." J. Mater. Civ. Eng. 26 (6): 04014014. https://doi.org/10.1061/(ASCE)MT.1943-5533.0000953.
- Whang, D. H. 2001. "Seismic compression of compacted soils." Ph.D. dissertation, Dept. of Civil and Environmental Engineering, Univ. of California.
- Wu, J. 2002. "Liquefaction triggering and post-liquefaction deformation of Monterrey 0/30 sand under uni-directional cyclic simple shear loading." Ph.D. dissertation, Dept. of Civil and Environmental Engineering, Univ. of California.
- Wu, J., A. M. Kammerer, M. F. Riemer, R. B. Seed, and J. M. Pestana. 2004. "Laboratory study of liquefaction triggering criteria." In *Proc.*, 13th World Conf. on Earthquake Engineering, 2580. Vancouver, BC, Canada: Canadian Association for Earthquake Engineering.
- Yoshimine, M., H. Nishizaki, K. Amano, and Y. Hosono. 2006. "Flow deformation of liquefied sand under constant shear load and its applications to analysis of Flow slide in infinite slope." Soil Dyn. Earthquake Eng. 26 (Feb): 253–264. https://doi.org/10.1016/j.soildyn.2005.02.016.
- Youd, T. L. 1972. "Compaction of sands by repeated shear straining." J. Geotech. Eng. Div. 98 (7): 709–725. https://doi.org/10.1061/JSFEAQ .0001762.
- Zhang, G., P. K. Robertson, and R. W. I. Brachman. 2002. "Estimating liquefaction-induced ground settlements from CPT for level ground." Can. Geotech. J. 39 (4): 1168–1180. https://doi.org/10.1139/t02-047.